FG.

AFWL-TR-74-338

(12)

AFWL-TR-74-338

ADA022260

SELF-CONSISTENCY AND RADIATION ENHANCED GROUND CONDUCTIVITY IN THE SURFACE BURST CODE SCX

Science Applications Corporation
La Jolla, CA 92037

November 1975

Final Report

Approved for public release; distribution unlimited.

This research was sponsored by the Defense Nuclear Agency under Subtask R99QAXEA094, Work Unit 41, Work Unit Title: Low Altitude Predictions.

Prepared for
Director
DEFENSE NUCLEAR AGENCY
Washington, DC 20305

AIR FORCE WEAPONS LABORATORY
Air Force Systems Command
Kirtland Air Force Base, NM 87117

388 862

AFWL-TR-74-338

This final report was prepared by the Science Applications Corporation, LaJolla, California under Contract F29601-74-C-0006, Job Order WDNE0707 with the Air Force Weapons Laboratory, Kirtland Air Force Base, New Mexico. Capt. William A. Seidler (ELP) was the Laboratory Project Officer-in-Charge.

When US Government drawings, specifications, or other data are used for any purpose other than a definitely related Government procurement operation, the Government thereby incurs no responsibility nor any obligation whatsoever, and the fact that the Government may have formulated, furnished, or in any way supplied the said drawings, specifications, or other data is not to be regarded by implication or otherwise as in any manner licensing the holder or any other person or corporation or conveying any rights or permission to manufacture, use, or sell any patented invention that may in any way be related thereto.

This technical report has been reviewed and is approved for publication.

WILLIAM A. SEIDLER
Capt, USAF
Project Officer

FOR THE COMMANDER

LARRY W. WOOD
LtCol, USAF
Chief, Phenomenology and
Technology Branch

JOHN W. SWAN
Colonel, USAF
Chief, Electronics Division

This report has been reviewed by the Information Office (OI) and is releasable to the National Technical Information Service (NTIS). At NTIS, it will be available to the general public, including foreign nations.

DO NOT RETURN THIS COPY. RETAIN OR DESTROY.

UNCLASSIFIED

SECURITY CLASSIFICATION OF THIS PAGE (When Data Entered)

REPORT DOCUMENTATION PAGE

READ INSTRUCTIONS BEFORE COMPLETING FORM

1. REPORT NUMBER AFWL-TR-74-338	2. GOVT ACCESSION NO.	3. RECIPIENT'S CATALOG NUMBER
4. TITLE (and Subtitle) SELF-CONSISTENCY AND RADIATION ENHANCED GROUND CONDUCTIVITY IN THE SURFACE BURST CODE SCX.		5. TYPE OF REPORT & PERIOD COVERED Final Report. 6. PERFORMING ORG. REPORT NUMBER SAI-74-505-AQ
7. AUTHOR(s) B. H. Fishbine, S. J. Dalich & J. N. Wood		8. CONTRACT OR GRANT NUMBER(s) F29601-74-C-0006 NEW
9. PERFORMING ORGANIZATION NAME AND ADDRESS Science Applications Corp. 1200 Prospect Street, P.O. Box 2351 LaJolla, CA. 92037		10. PROGRAM ELEMENT, PROJECT, TASK AREA & WORK UNIT NUMBERS 62707H, WDNE 0707 Subtask: R99QAXEA094 Work Unit: 41
11. CONTROLLING OFFICE NAME AND ADDRESS Director Defense Nuclear Agency Washington, DC 20305		12. REPORT DATE November 1975 13. NUMBER OF PAGES 54
14. MONITORING AGENCY NAME & ADDRESS(if different from Controlling Office) Air Force Weapons Laboratory Air Force Systems Command Kirtland AFB, NM 87117 12 44p.		15. SECURITY CLASS. (of this report) Unclassified 15a. DECLASSIFICATION/DOWNGRADING SCHEDULE

16. DISTRIBUTION STATEMENT (of this Report)

Approved for public release; distribution unlimited.

17 A094 16 DNA-NWET-QAXE

17. DISTRIBUTION STATEMENT (of the abstract entered in Block 20, if different from Report)

18. SUPPLEMENTARY NOTES

This research was sponsored by the Defense Nuclear Agency under Subtask R99QAXEA094, Work Unit 41, Work Unit Title Low Altitude Predictions.

19. KEY WORDS (Continue on reverse side if necessary and identify by block number)

Electromagnetic Pulse (EMP)
High Altitude EMP
EMP Code Development
EMP Prediction Techniques

20. ABSTRACT (Continue on reverse side if necessary and identify by block number)

A description of the numerical techniques used to include the self-consistent effect in the two-dimensional ground burst EMP code, SCX, is given. The effect of this phenomenon on the fields predicted by SCX is discussed and illustrated. The effect is most notable for observer positions less than 2,000 meters from the burst point where a sign change occurs in the transverse E field.

Next Page

DD FORM 1 JAN 73 1473 EDITION OF 1 NOV 65 IS OBSOLETE

UNCLASSIFIED

SECURITY CLASSIFICATION OF THIS PAGE (When Data Entered)

Also presented are discussion and results concerning the inclusion of a radiation enhanced ground conductivity model in SCX. Results of calculations with this model indicate that for a zero height of burst situation, field effects are minimal.

TABLE OF CONTENTS

LIST OF FIGURES

LIST OF FIGURES (Continued)

SECTION I
INTRODUCTION

SCX is a two dimensional ground burst EMP (electromagnetic pulse) computer code. The general numerical methods used in the code are documented(1) elsewhere and will not be discussed here. Briefly, the code obtains the solution to Maxwell's equations in the source region of a surface nuclear burst. Because the solution is obtained in the source region, several nonlinearities are inherent to the problem. First, the conductivity of the medium depends strongly on the total electric field. The effect has always been modeled in the code. Second, the source terms are themselves influenced by the fields. This effect is generally referred to as "self-consistency", and until recently was not included in the SCX code. This paper reviews the methods used to model self-consistency in SCX, and presents comparative results of calculations before and after the effect was included in SCX.

An exact representation of self-consistency requires the solution to the equations of motion for the Compton electrons. Clearly, for an EMP computer code with two space dimensions plus time, this is impractical. The amount of storage required is not available, and the running time would render the code economically useless. Fortunately, methods have been devised which allow for the inclusion of the self-consistent effect in an approximate fashion(2). These methods require a minimal amount of storage and cause only slight increases in running time.

The sources of the EMP are the Compton recoil electrons created through the device radiation interactions with the atmosphere. In SCX these sources are described as current densities in the radial and transverse directions. The current densities were obtained from Monte Carlo transport calculation results which were then curve fit for use in the code. The transport results, being completely independent of the EMP calculation, do not contain any effects due to interactions with

electromagnetic fields. To include the self-consistent effect, some modification must be made to the source terms within the SCX code. This leads to several necessary approximations, the impact of which will be discussed below.

SECTION II
A DESCRIPTION OF THE SELF-CONSISTENCY MODEL

The self-consistency model used is derived from EMP Theoretical Note 77, Volume 2-4, by H. J. Longley.[2] The note describes a way of modifying a purely radial, analytic current source to obtain self-consistent radial and transverse currents. The method is based on electron turning in the presence of electromagnetic fields.

To determine the amount of turning, a group of electrons is followed in various time constant electromagnetic environments. These electrons are recoils created by Compton scattered, monoenergetic gamma rays and are chosen to represent a physically realistic distribution of Compton recoil angles and energies. The equations of motion for the electrons are differenced and solved numerically. The computation proceeds in time until an electron's kinetic energy is within 1% of its rest mass energy. In STP air, 1 MeV electron has a range of .49 g/cm^2. An electron with a kinetic energy equal to 10% of [illegible] rest mass energy, has a range of .0049 g/cm^2. So a 1 MeV el[illegible]on slowed to 1% of its rest mass energy is easily within .1% of its final range. At this point, the electron's final radial and transverse positions are recorded. An average is taken of the final positions for the group of electrons and these averages are used to obtain self-consistent currents. The validity of this method depends on the lifetimes of the electrons and the time steps used in the SCX calculation. This matter will be discussed later.

To obtain the self-consistent radial current, the original radial, analytic current is multiplied by DX/R_{mf} where DX is the average electron final radial position and R_{mf} is the mean forward range of the electron in the absence of fields. The self-consistent transverse current is obtained by multiplying the original radial current by DY/R_{mf}, where DY is the average electron final transverse position. In the earth's magnetic field, the Larmor radius of a 1 MeV electron is about 100 times

its range. Since typical EMP fields produce much greater effects, such as reversing the transverse current obtained from Monte Carlo transport calculations, the geomagnetic field will be neglected.

Two items are important in this method. The first is the initial kinetic energy, E_e, of an electron to be tracked. This energy depends on the initial gamma energy, $E_{\gamma o}$, and the scattering angle and is obtained directly from the Klein-Nishina equation. The second item of importance is the calculation of R_{mf}. R_{mf} is the mean forward range obtained by

$$R_{mf} = \frac{1}{\sigma_c} \int_{\theta_e = 0}^{\pi/2} R \cos \theta_e \sigma_e d\Omega_e \tag{1}$$

where

$$\sigma_c = \int_{\theta_e = 0}^{\pi/2} \sigma_e d\Omega_e \tag{2}$$

and σ_e is the angular differential cross-section obtained from the Klein-Nishina formula, $d\Omega_e$ is the solid angle associated with the scattering angle θ_e of the recoil electron, θ_e is the angle between the initial direction of propagation of the gamma and the direction of the electron's recoil. R is the range obtained from a fit to experimental mean range versus energy data. The energy used to obtain R is E_e which is a function of $E_{\gamma o}$ and θ_e.

Our method of obtaining self-consistent currents is different in several respects from the method described in EMP Theoretical Note 77. Where Longley's method used only an analytic, radial current source; the current sources used in SCX have both radial and transverse components. The general method described in Note 77 is designed for use with an analytic current source. The source terms in SCX are, however, not analytic, having been obtained through curve fits to the results of gamma and neutron Monte Carlo transport calculations. The source terms serve as inputs to SCX, and are expressed

as total currents in the radial and transverse directions. In order to adapt the general method to our purposes, tables similar to Longley's were generated. However, our tables are for electrons recoiling in the same direction as the initial gamma propagation direction and are not averages of electrons recoiling at different θ_e. This was done because the transport calculations which provide the current sources for SCX already include angular scatter effects and the electron energy spectrum is already folded in.

In applying DX/R and DY/R factors to the SCX transport derived currents, first a total initial current is calculated from the initial transport derived radial and transverse currents. This total current is then treated in the same manner that the analytic radial current source is treated in Longley's method. To accomplish this, the angle between the positive radial axis and the total initial current is used to transform the radial and transverse electric fields to a new primed coordinate system where the total initial current is parallel to the primed positive radial axis (i.e., a transformation to a coordinate system in which the transverse current is zero). The DX/R and DY/R factors are applied to the total initial current and the resulting primed self-consistent radial and transverse currents are transformed back to the original coordinate system to obtain the final self-consistent currents.

In addition to following single electrons rather than probabilistically representative groups, our method differs from Longley's in two respects. First, rather than using the initial electron kinetic energy calculated directly from the Klein-Nishina equation, a mean initial electron energy is used. This energy is calculated by

$$\overline{E}_e = \frac{1}{\sigma_c} \int_{\theta_e=0}^{\pi/2} E_e \sigma_e \, d\Omega_e$$

Where E_e is a function of θ_e and initial gamma energy, $E_{\gamma o}$, and is calculated from the Klein-Nishina equation.

Secondly, the range we use is different from R_{mf}, the mean forward range used by Longley. We use a range R_c, which is the electron range calculated by the electron tracking subroutine with all fields set to zero. This range differs from the range obtained by using $\bar{E}_e$ and the R in Eqn. (1) only because of roundoff error.

In Longley's scheme, tables of DX and DY were generated for various field values and gamma energies. These tables were then fit by analytic functions and the functions used to introduce self-consistency into the LEMP code. In our case, tables of DX/R_c and DY/R_c are generated and used directly by SCX, along with some interpolation coding, to obtain self-consistency. The interpolation scheme is simple-minded and chosen to supply smooth sources to SCX.

The interpolation is basically as follows. The three field values calculated by SCX are the radial electric field (E_r), the transverse electric field (E_θ) and the phi magnetic field (B_ϕ). These fields can be thought of as the three coordinates of a field space. For the DX/R_c tables each entry in the table represents a point in the field space. Similarly for DY/R_c. For a given set of field values calculated by SCX, the interpolation coding determines what eight points, the vertices of a rectangular solid, corresponding to given DX/R_c or DY/R_c surround the point P whose coordinates are given by the three field values. This rectangular solid can be broken up into eight sub-solids by passing three planes through the fields value point. The planes are parallel to the six faces of the original solid and generate one sub-solid for each vertex of the original solid. The interpolation scheme weights the DX/R_c or DY/R_c value at a particular vertex by a volume obtained by subtracting the volume of the sub-solid of that vertex from the volume of the original solid. This weighting is done for all eight points, summed and divided by the total volume of the original solid. The scheme is smooth and has the advantage

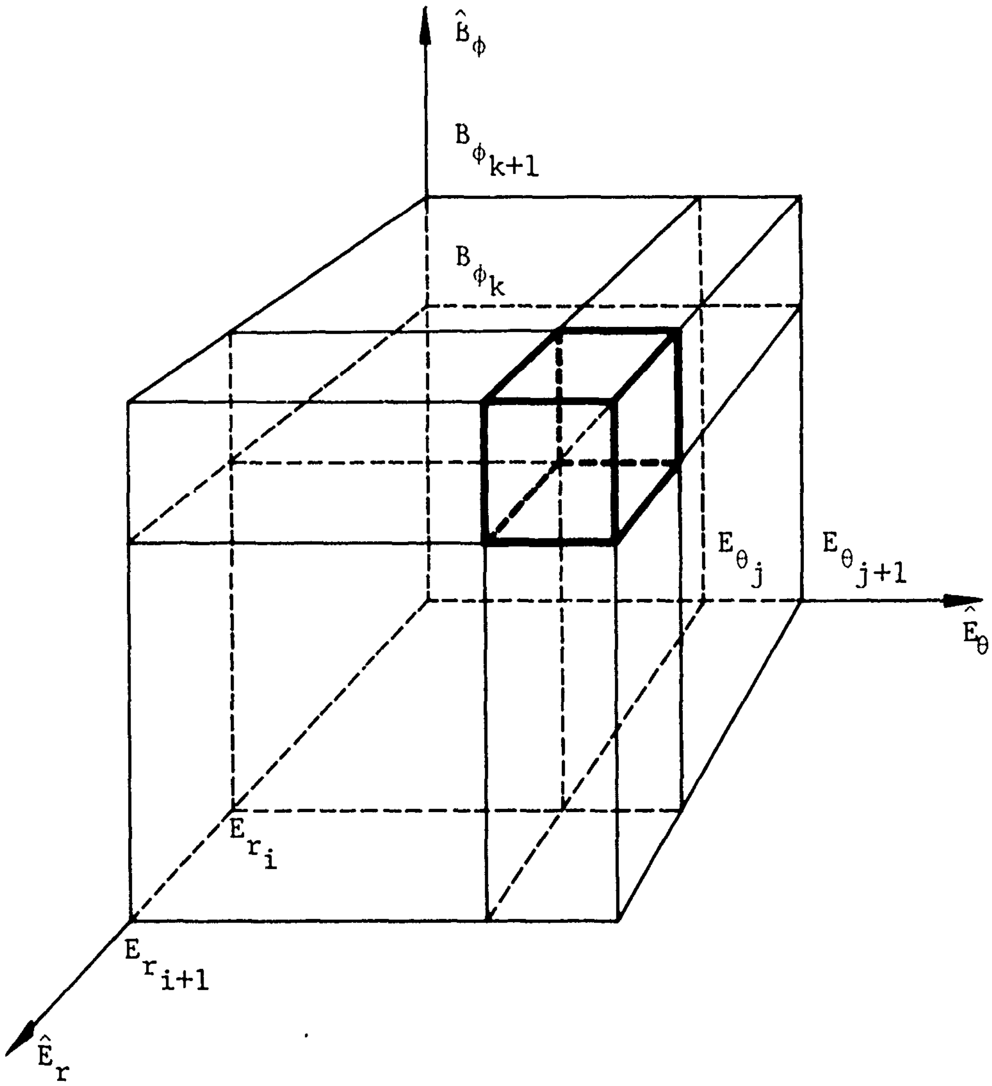

Fig. 1. The field space used in the interpolation scheme.

that if the fields values fall exactly on a point in the tables, the precise values of DX/R_c and DY/R_c from the tables are obtained.

The equation of motion used in the electron tracker subroutine is:

$$\dot{\vec{p}} = -|e| \left\{ \vec{E} + \vec{v} \times \vec{B} \right\} - A \frac{\vec{p}}{|\vec{p}|}$$

where $\vec{p}$ is the electron's momentum, e the electron's charge, $\vec{v}$ the electron's velocity, $\vec{E}$ the electrical intensity of the environment, $\vec{B}$ the magnetic intensity, and A is a slowing term like $\frac{dE}{ds}$ which includes energy losses due to ionization, multiple scattering and radiation. If $\vec{E}$ and/or $\vec{B}$ are large enough their contributions will overcome the energy loss term A and the electrons will never come to rest. These are termed run-away electrons. The self-consistency model used here includes a range of field values which generate DX/R_c and DY/R_c tables that exclude run-away electrons. Therefore, the interpolation coding holds field values to the limits used in generating the tables.

In estimating the effect of self-consistency on the conductivity we have to consider the effects of the electric fields on an electron's kinetic energy, since the kinetic energy determines the amount of ionization. If an electron has an initial velocity in a given direction an electric field parallel to the velocity vector will increase or decrease the electron's kinetic energy depending on the sign of the field.

Generally, the direction of the radial electric field is positive, away from the burst source point. Similarly for the Compton recoil electrons. Therefore, the radial electric field tends to reduce the recoil electron energy and thereby reduce the ionization due to electrons. Initially the theta electron velocity in the transformed system is zero so that the theta electric field will increase the electron's theta momentum

regardless of the field's sign. These approximate arguments lead 3 to the following correction factor, f_q, to the ionization rate.

$$f_q = \frac{\bar{E}_e + W}{\bar{E}_e}$$

where

$$W = |e| \left\{ |E_\theta DY| - E_r DX \right\}$$

and $|e|$ is the absolute value of the electron's charge. W is an estimate of the work done by the fields on the electron and therefore changes the energy available for ionization.

The applicability of this self-consistent scheme is questionable when the time steps used by fields code differencing are comparable or less than the lifetimes of the electrons. In real time, for gammas of 1.5 MeV, electron lifetimes are on the order of 10^{-8} second. In retarded time, due to turning, this time may be much larger since there is a component of the electron velocity which is parallel to the gamma wave front.

In a typical SCX run, the time steps during the prompt gamma peak are 10^{-9} second. After the peak, time steps are 10^{-8} second and larger. By examining electron trajectories for typical SCX environments it is apparent that the electrons frequently turn back and complete loops. But it is still likely that the final position of an electron is in the same general direction from the electron's original position as the position of an electron at the end of a time step shorter than the electron's lifetime. Since the electron is slowing down, we expect that the electric fields, at least, will have more effect on the electron's position near the end of its life than at the beginning where it has large kinetic energy. In the present SCX calculations, the self-consistent effect is probably exaggerated during the prompt gamma peak.

An approximate correction in such situations might be to scale the turning by a factor $t_s/t_{e\ell}$, where t_s is the time step and $t_{e\ell}$ is the electron lifetime. A better factor would be

$$f_t = (t_s/t_{e\ell})^2$$

which more heavily weignts time steps close to $t_{e\ell}$. The f_t factor is plausible because the non-relativistic equation for a displacement s due to a constant force on a mass m is

$$s = \frac{F}{2m} t^2 .$$

The f_t factor would scale the angle that the position vector of the electron's final position makes with the initial gamma propagation direction. To accomplish this, take the original DX/R_c and DY/R_c. Compute

$$\alpha = \left\{[DY/R_c] \; / \; [DX/R_c]\right\} = \tan \delta$$

$$m = \left\{[DX/R_c]^2 + [DY/R_c]^2\right\}^{\frac{1}{2}}$$

$$\beta = \arctan \left\{\alpha \cdot f_t\right\}$$

$$[DX/R_c]' = m \cos (\beta)$$

$$[DY/R_c]' = m \sin (\beta)$$

and use $[DX/R_c]'$ and $[DY/R_c]'$ as before.

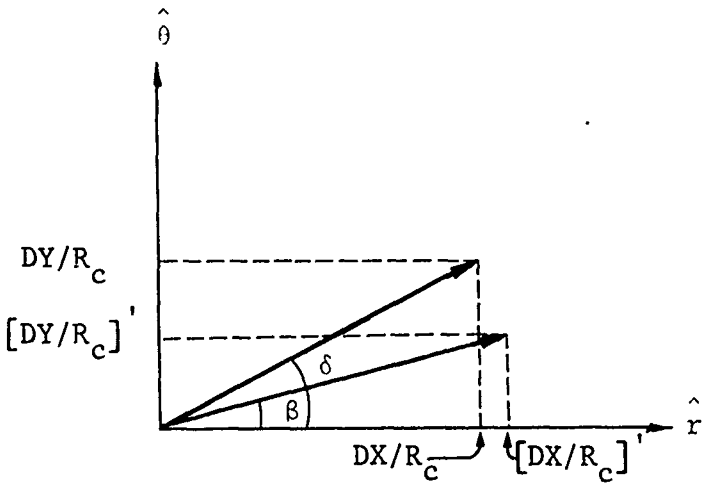

Fig. 2. Scaling Self-Consistent Currents by the Time-Step Factor.

SECTION III
THE EFFECT OF SELF-CONSISTENCY ON THE CURRENTS

To interpret the plots overlaying self-consistent and non-self-consistent time histories of SCX runs, it is useful to first describe the individual effects of the fields on a single electron.

For an electric field $\vec{E}$, the force on a charge q is $\vec{F} = \vec{E}\,q$. An electron in a positive E_r field experiences a force in the $-\hat{r}$ direction which contributes to a positive radial conventional current. Since the Compton recoil electrons are streaming radially outward, constituting a negative conventional current, the isolated effect of a positive E_r field is to reduce the magnitude of the negative radial current $-J_r$. The same type of argument indicates the effect of E_θ on the theta current.

SCX calculates a B_ϕ which is negative. Since $|J_r|$ is usually greater than $|J_\theta|$, we first consider the effect of a magnetic field on a purely radial current.

An electron with a velocity $\vec{v}$ in the $+\hat{r}$ direction will experience a magnetic force $\vec{F} = q(\vec{v} \times \vec{b})$. For B_ϕ negative $\vec{F}$ will be in the $-\hat{\theta}$ direction and so contribute to a positive theta conventional current.

Occasionally, J_r and J_θ are the same order of magnitude. In the extreme case where the conventional current is purely in the $-\theta$ direction, the magnetic field will contribute to a negative radial conventional current.

In determining whether it is an electric field or the magnetic field which dominates the electron turning, it is useful to be able to make rough comparisons between the effects of the electric and magnetic fields.

For an electron of initial energy $\overline{E}_e$, initial speed v_o, and absolute charge e, we define F_m to be the maximum magnetic force on the electron and F_s to be the maximum slowing force on the

electron. Since these two forces are monotonically increasing functions of the electron velocity, (except for F_s when the electron energy is below 0.5 MeV) the maxima occur at the electron's maximum speed, i.e., v_o. For an incident gamma of 1.5 MeV, E_e is .75 MeV and v_o is 2.75×10^8 m/sec. F_m and F_s can then be compared as follows:

$$F_m/e = B_\phi \cdot 2.75 \times 10^8$$

$$F_s/e = \frac{A(v)_o}{e} = 3.49 \times 10^5$$

The slowing term $A(v_o)$ is obtained from a fit to experimental data of electron energy as a function of electron mean range. This fit is differentiated with respect to range to obtain $\frac{dE}{ds}$.

With the use of F_m and F_s we can predict the combination of effects of the various fields on the currents.

The radial current overlays in Figs. 3 and 12 show that for ranges of 500m and 1000m the self-consistent model reduces the magnitude of the radial current until past a microsecond. This is especially noticeable at the time of the prompt gamma peak and also past 10 shakes where the reduction in J_r increases markedly with time until near a microsecond. The 2000m radial currents overlay exactly, which prompts us to consider the close-in ranges and the 2000m range separately. Evidently, at 2000m for this yield, the fields are reduced enough to show only small self-consistent effects, primarily in J_θ and E_θ.

As mentioned earlier, the effect of a positive E_r field is to reduce the magnitude of a negative J_r. For the two close-in ranges, E_r is positive throughout the calculation. Also, a negative B_ϕ will only increase the magnitude of negative J_r when J_θ is negative and $|J_\theta| \sim |J_r|$. In the self-consistent case, we see that $|J_r|/|J_\theta|$ is close to unity at 1½ μsec. At this point, in Fig. 3, the self-consistent J_r is increased as expected. By comparing the

non-self-consistent J_θ and J_r, it is seen that separation between the self-consistent J_r and non-self-consistent J_r continues to increase.

The more pronounced $-J_r$ reduction at the time of the prompt gamma peak is due to the combined peaking of E_r and B_ϕ. After the prompt gamma pulse, whereas E_r is saturated and remains reasonably constant out to neutron arrival at around 10 microseconds, B_ϕ steadily increases in magnitude and thus increases the separation of the J_r overlays. It is interesting to note that at 500m the self-consistent B_ϕ starts leveling off at around 2 μsec and then starts to decrease at about 5 μsec. The separation in the J_r overlays follows this behavior until the non-self-consistent J_θ becomes larger than the non-self-consistent J_r. Similar behavior is shown at 1000m.

At 2000m there is no visible effect of the self-consistent model on the radial current. This is plausible on the basis of rough field comparisons. The maximum value of E_r at this range is 5×10^3. The maximum absolute value of B_ϕ is 3×10^{-4}. In this case, F_m/e is $\sim 8 \times 10^4$. Since F_s/e is $\sim 3.5 \times 10^5$, it seems reasonable that the self-consistent effect on J_r due to E_r will be negligible, and the effect due to B_ϕ will be small, particularly since at this range, $|J_r| >> |J_\theta|$ and nearly all the kinetic energy of the electron is in the radial direction.

The self-consistent theta currents for the two close-in ranges show three interesting features. First, while the non-self-consistent theta currents are always negative, the self-consistent theta currents are nearly always positive. Second, the self-consistent theta currents follow the prompt gamma pulse in a much more obvious fashion than the non-self-consistent theta currents. Third, after the prompt gamma pulse, the self-consistent theta currents dip and then exhibit a gentle bump, and finally change sign after 10 microseconds.

The self-consistent theta currents are nearly always positive because B_ϕ nearly always predominates over E_θ and the non-self-consistent J_r is nearly always greater than the non-self-consistent

J_θ. There is a very short span of time at very early times where E_θ predominates. If values of E_θ and F_m/e are compared at 3 shakes in the usual manner, the E_θ dominance can be shown. In this tiny region of E_θ dominance, the self-consistent theta currents are negative. This situation is shown in Figs. 5 and 14.

That the theta currents are almost entirely determined by B_ϕ is further demonstrated by the jagged time behavior of E_θ and consequent smearing of the prompt gamma pulse. In contrast, the theta currents are smooth and follow the gamma pulse quite well because close-in the shape of the gamma pulse is preserved in B_ϕ.

Finally, the dip and gentle bump behavior is exhibited in B_ϕ but, due to the obvious non-linear relationship of electron turning to the magnitude of B_ϕ, the similarity of shape between the self-consistent J_θ and B_ϕ is not compelling, especially as the waveforms approach 10 μsec where the non-self-consistent J_θ becomes comparable to or greater than the non-self-consistent J_r. Beyond 10 μsec J_θ crosses over due to the fact that the non-self-consistent J_θ becomes comparable to or greater than (at 500m) the non-self-consistent J_r. In this region the effect of B_ϕ is to increase - J_r, as explained above, and so E_θ dominates J_θ behavior. E_θ starts its dominance before 10 μsec. The effect is to reverse J_θ. At 12 μsec and 500m (Fig. 9) and 22 μsec and 1000m (Fig. 18) E_θ crosses over and becomes positive. This causes the self-consistent J_θ to hump over as it heads for another cross-over.

At 2000m, rough field comparison shows that E_θ should dictate J_θ behavior. First, a vestige of the gamma pulse is seen in J_θ. The shape of the gamma pulse is preserved in E_θ but not in B_ϕ. Second, J_θ is uniformly negative as is E_θ past the start of the gamma pulse. Later in time B_ϕ rises faster than E_θ and at its peak there is a corresponding dip in J_θ because, as shown earlier, a negative B_ϕ acting on a negative J_r contributes to a positive J_θ.

Now it remains to examine the effects of the self-consistent model on the fields and the conductivity.

SECTION IV
THE EFFECT OF SELF-CONSISTENCY ON THE FIELDS

A few words should be said regarding the occasional raggedness of some of the fields. By examining range plots of E_θ, it is clear that choosing the inner boundary condition $E_\theta = 0$ is inappropriate. Originally this condition was chosen with the assumption that the inner boundary is a perfect conductor. This assumption is certainly inconsistent with the use of non-zero theta currents at the inner boundary. Range plots of E_θ at early times show a drastic discontinuity between the inner boundary and the first point out in range. In fact, E_θ is increasing in an exponential fashion toward the inner boundary rather than decreasing to zero. After a few time steps, this discontinuity develops into oscillations of E_θ in range. In turn these oscillations affect J_θ which feeds back into E_θ. To minimize these oscillations, a range current smoother has been installed in SCX. This stopgap measure is helpful but not completely effective as can be seen in the time plots o' near the prompt gamma pulse.

In addition, the calculation of the conductivity involves using a field dependent electron mobility which is clearly affected by the erratic behavior of E_θ. The conductivity's slightly ragged behavior is fed back into E_r and into B_ϕ. This problem should be cleared up, if not eliminated, by a more physically realistic choice of inner boundary condition for E_θ, possibly something as simple-minded as:

$$E_\theta = -J_\theta/\sigma$$

The three equations of importance in SCX are, in retarded time, at $\theta = 90^\circ$ (on the ground)

1) $$\frac{1}{\mu r}\frac{\partial B_\phi}{\partial \theta} = J_r + \sigma E_r + \varepsilon_o \frac{\partial E_r}{\partial \tau}$$

2) $$-\frac{1}{\mu r}\left[\frac{\partial}{\partial r}(rB_\phi) - \frac{1}{c}\frac{\partial}{\partial \tau}(rB_\phi)\right] = J_\theta + \sigma E_\theta + \varepsilon_o \frac{\partial E_\theta}{\partial \tau}$$

3) $$\frac{1}{r}\left[\frac{\partial}{\partial r}(rE_\theta) - \frac{1}{c}\frac{\partial}{\partial \tau}(rE_\theta) - \frac{\partial}{\partial \theta}E_r\right] = -\frac{\partial B_\phi}{\partial \tau}$$

The usual arguments used to predict the time behavior of E_r from 1) are as follows. With the magnetic term negligible, at very early times J_r, σ and E_r are very small and so σE_r is negligible relative to J_r. Hence, the E_r behavior is predicted to be: $E_r = -\frac{1}{\varepsilon}\int J_r d\tau$.

After a time, σE_r becomes comparable to $-J_r$. Physically, this is described as occurring when the Compton current is cancelled by the conduction current. When this condition occurs $\frac{\partial E_r}{\partial \tau}$ is negligible, assuming the effects of the airground asymmetry have not yet allowed B_ϕ to diffuse into the region of interest. If J and σ rise initially as $e^{\alpha t}$, E_r saturates, i.e., $\frac{\partial E_r}{\partial \tau}$ is small, for $\sigma > \alpha\varepsilon_o$, where ε_o is the free space permitivity. For an α of 2×10^8, saturation occurs where $\sigma > 1.77 \times 10^{-3}$ and the time of saturation can be determined by examining Figs. 6, 15 and 23. For 500 and 1000 meters, saturation occurs before the prompt gamma peak. At 2000 meters, saturation never occurs.

How accurately E_r follows $-J_r/\sigma$ is estimated by a "relaxation time" which amounts to ε_o/σ. If σ is large enough, the relaxation time is so short that E_r does in fact follow J_r/σ, most visibly at late times where J_r/σ changes. At far ranges or closer in at very late times, σ is so small that the relaxation time is too large to follow J_r/σ.

Furthermore, at the close-in ranges, 500 and 1000m, saturation occurs before the prompt gamma peak so that E_r also peaks, and at far ranges, 2000m, saturation occurs after the prompt gamma peak so that the peak is not preserved in E_r by following J_r/σ, but rather from $E_r = \frac{-1}{\varepsilon_0}\int J_r d\tau$. For E_r, this results in a peak more broad and delayed in time from the prompt gamma peak. In certain time domains, some of these arguments are equally applicable to E_θ.

At 500m and 1000m, saturation occurs before the prompt gamma peak. The plots of σ at these ranges show that the self-consistent model doesn't greatly change the conductivity. However, E_θ, through the field-dependent electron mobility, introduces some small jaggedness into σ.

Since $E_r = -J_r/\sigma$ until past neutron arrival where σ is greatly reduced, thus increasing the relaxation time, it is reasonable that the $1/\sigma$ dependence of E_r greatly exaggerates the jaggedness in σ. Since J_r is reduced by self-consistency, E_r is reduced as well.

An interesting portion of the E_r curve is at and past neutron arrival. The σ curves show a sharp discontinuity in slope at neutron arrival and a subsequent characteristic hump. E_r exhibits this same slope discontinuity and an inverted hump out to about 30 μsec.

Close in, before the prompt gamma peak, E_θ is driven by the $\frac{\partial}{\partial\tau}(rB_\phi)$ term. At 500m and 1000m, this can be readily seen. In both self-consistent and non-self-consistent plots of E_θ there is a very smooth, sharp negative pulse which peaks at about 5 shakes. If this pulse were due to $-J_\theta/\sigma$ the E_θ pulse caused by a self-consistent J_θ would be opposite in sign to the E_θ pulse generated by a non-self-consistent J_θ. Examination of the slope of the B_ϕ curve shows that the E_θ pulse is in fact driven by $\frac{\partial}{\partial\tau}(rB_\phi)$. Between 3 and 5 shakes, B_ϕ rises rapidly and smoothly to a peak. Since B_ϕ is negative, an increasing $\frac{\partial}{\partial\tau}(rB_\phi)$ should give a negative E_θ value. It is clear from the non-self-consistent plots of E_θ that the pulse ends and a

sign change occurs at the point where B_φ peaks and turns over. After B_ϕ peaks, the slope of B_ϕ doesn't dc anything of great interest until neutron arrival. In the intervening interval, E_θ is driven by $-J_\theta/\sigma$ as can be accurately verified by comparing $-J_\theta/\sigma$ with actual val s of E_θ.

An important difference shown in the overlay plots of E_θ at 500m and 1000m is that, whereas E_θ remains positive for a long time after the negative pulse for the non-self-consistent case, E_θ remains negative for the self-consistent case. Here E_θ is just following $-J_\theta/\sigma$.

At 2000m, an interesting feature is that while self-consistency reduces the magnitude of J_θ due to B_ϕ, the self-consistent E_θ is actually larger than the non-self-consistent E_θ at times greater than 10 shakes. Here E_θ is not driven by J_θ.

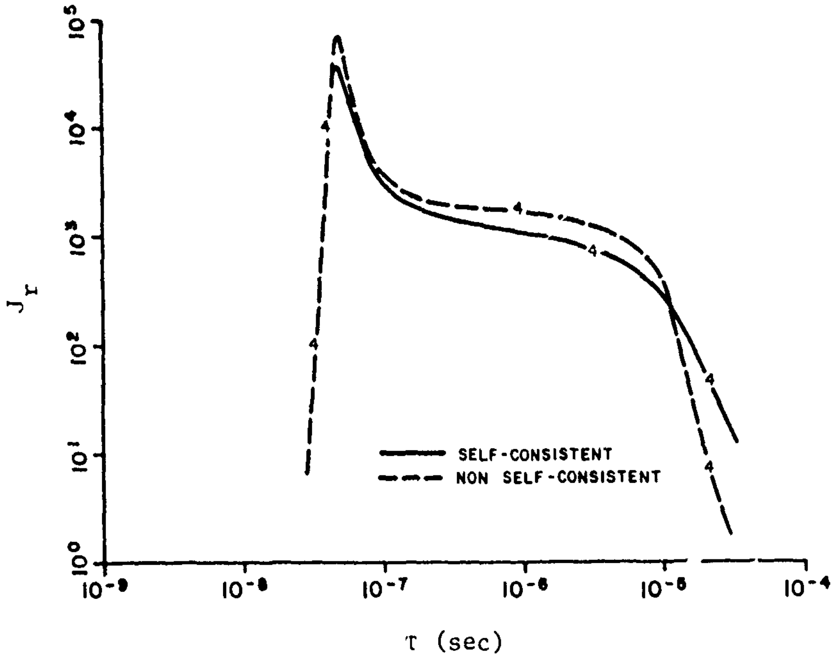

Fig. 3. Overlay of non-self-consistent and self-consistent radial currents at 500m, on the ground.

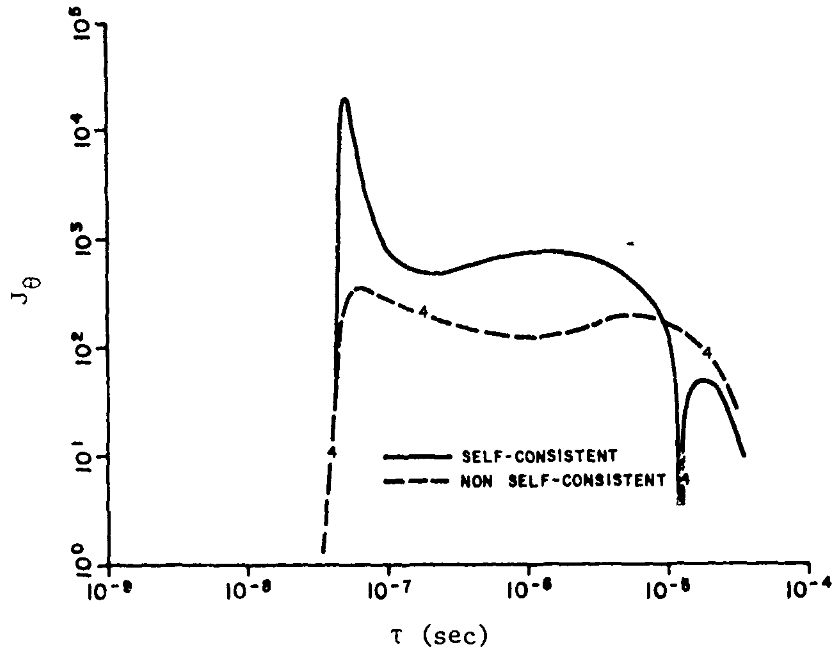

Fig. 4. Overlay, theta currents, 500m.

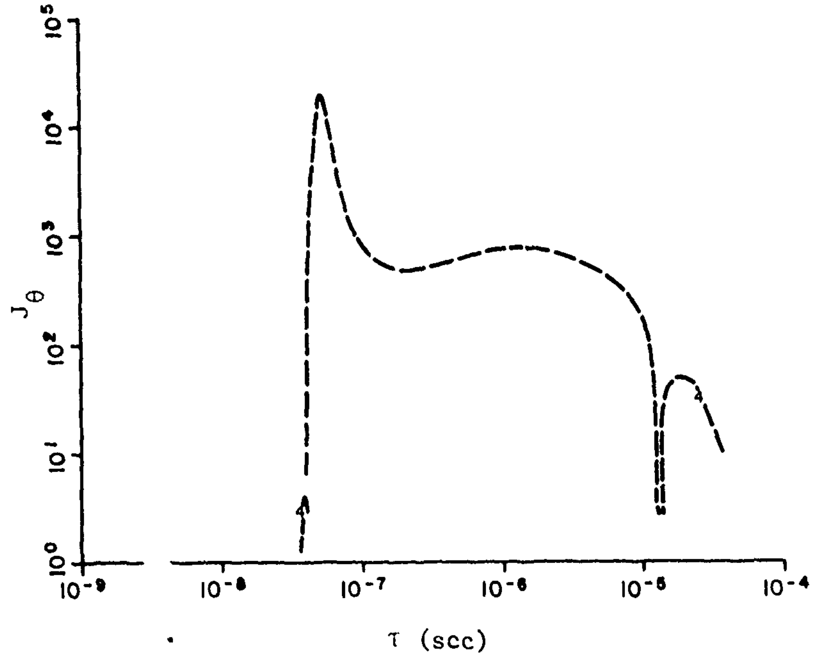

Fig. 5. Self-consistent theta current at 500m, on the ground.

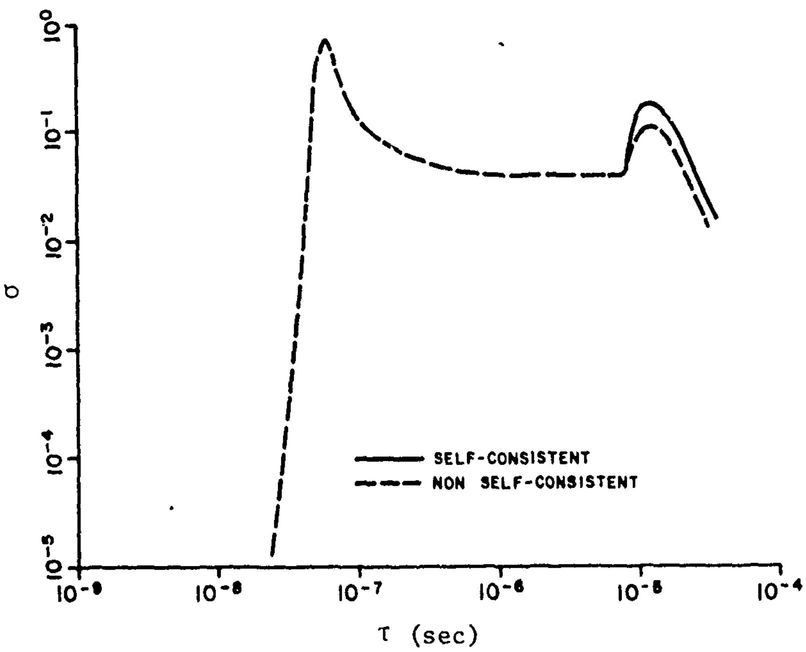

Fig. 6. Overlay, conductivities, 500m.

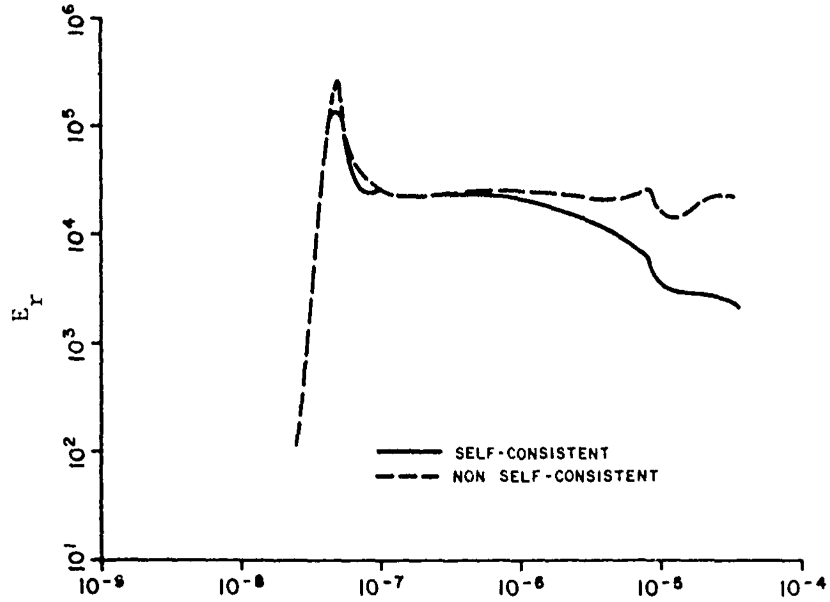

τ (sec)

Fig. 7. Overlay, radial electric fields, 500m.

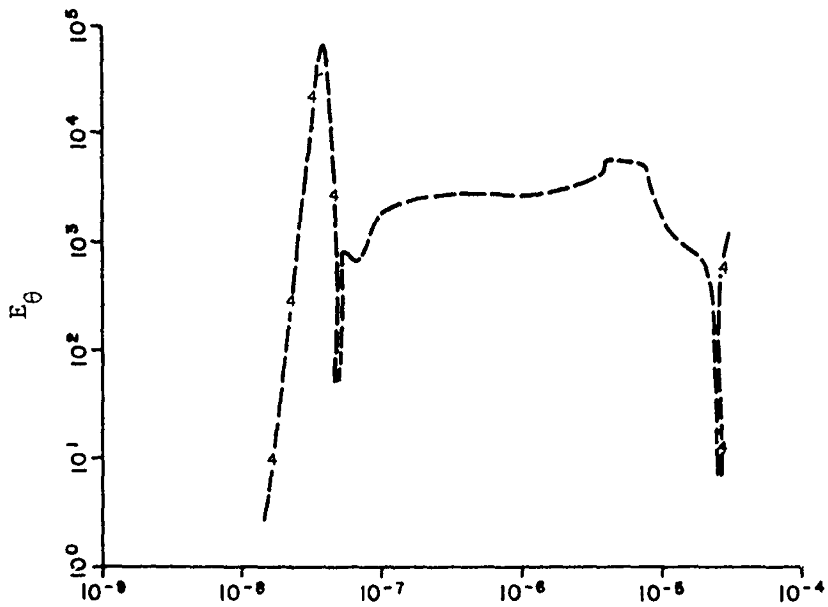

τ (sec)

Fig. 8. Non-self-consistent theta electric field at 500m, on the ground.

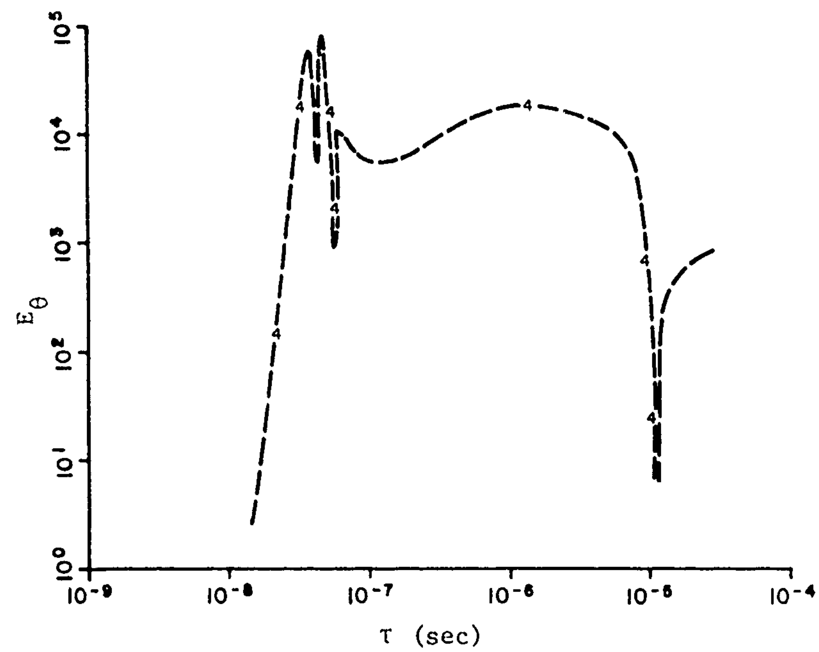

Fig. 9. Self-consistent theta electric field at 500m, on the ground.

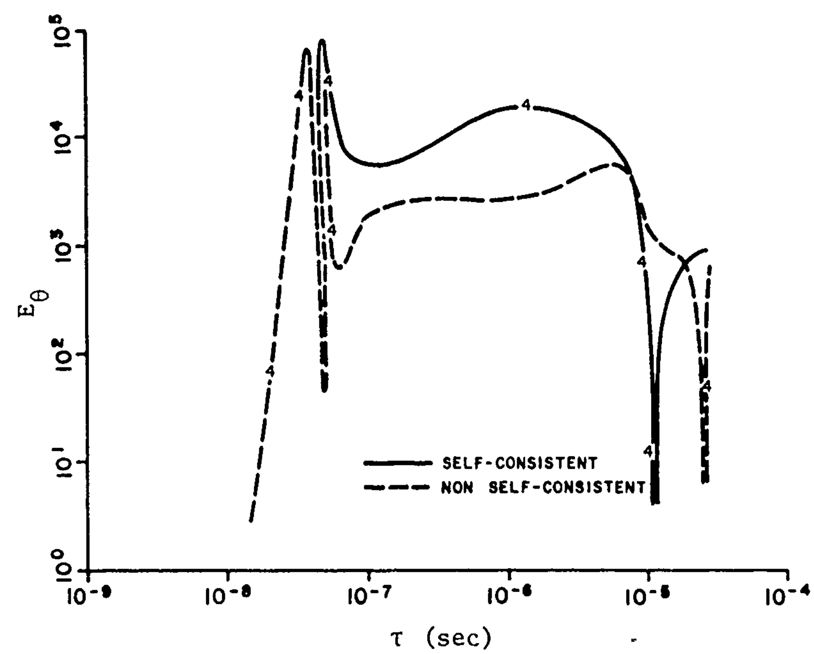

Fig. 10. Overlay, theta electric fields, 500m.

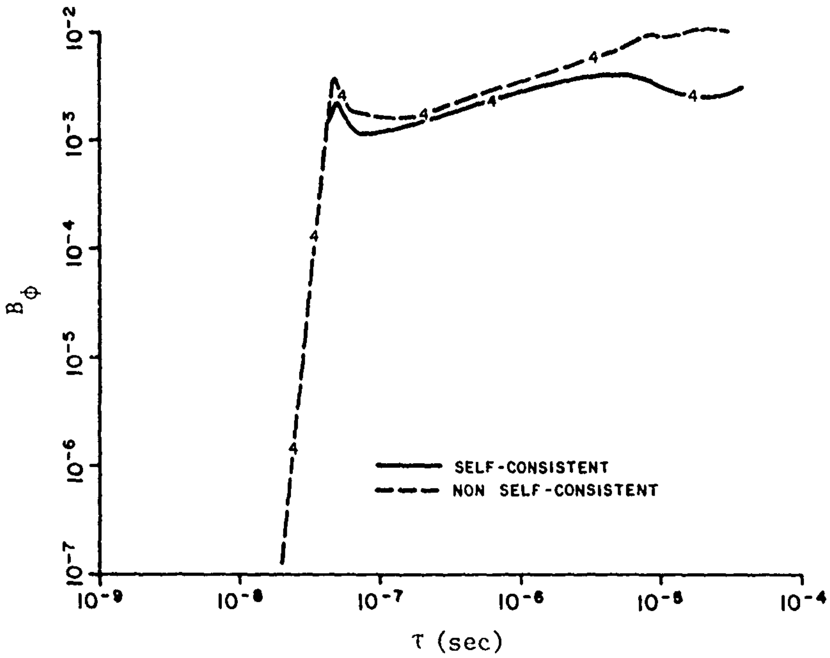

Fig. 11. Overlay, axial magnetic field, 500m.

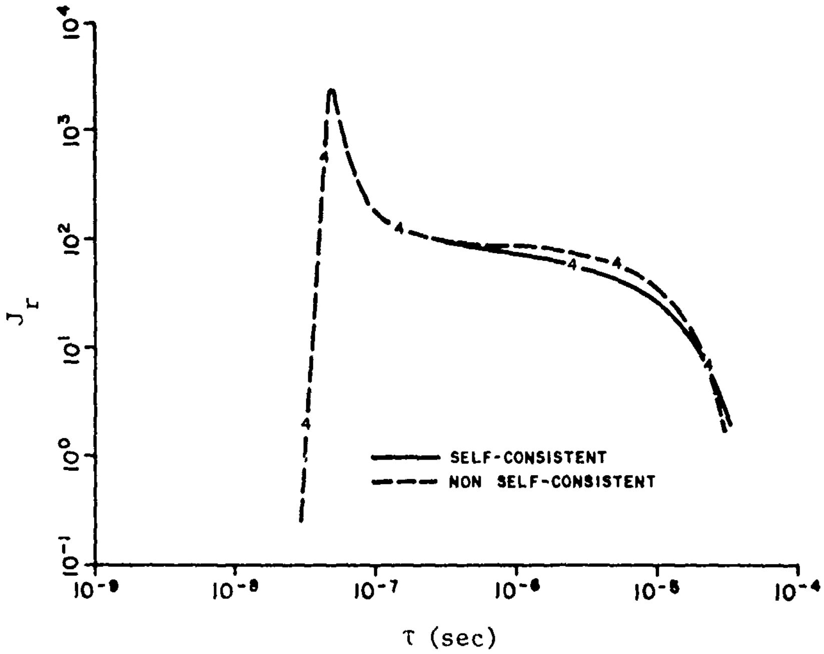

Fig. 12. Overlay, radial currents, 1000m.

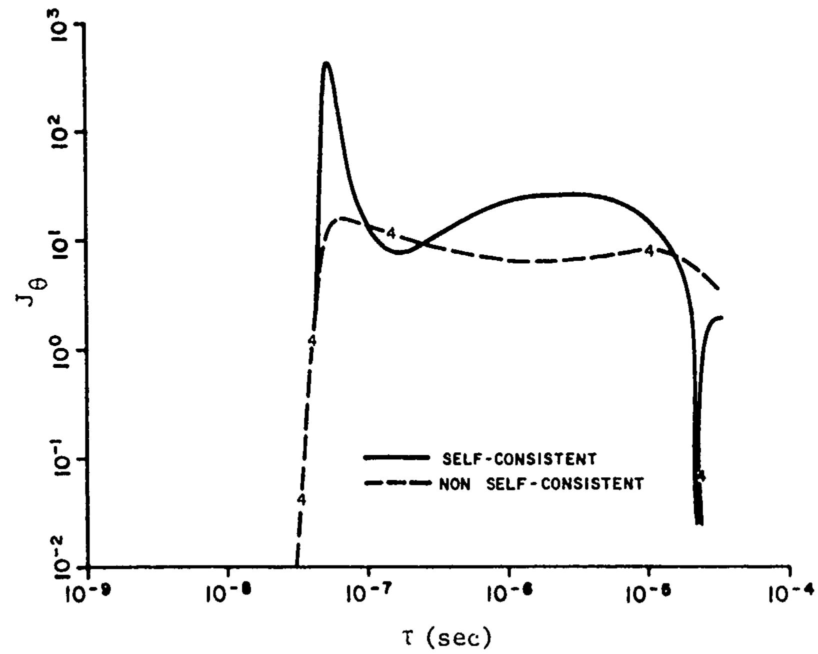

Fig. 13. Overlay, theta currents, 1000m.

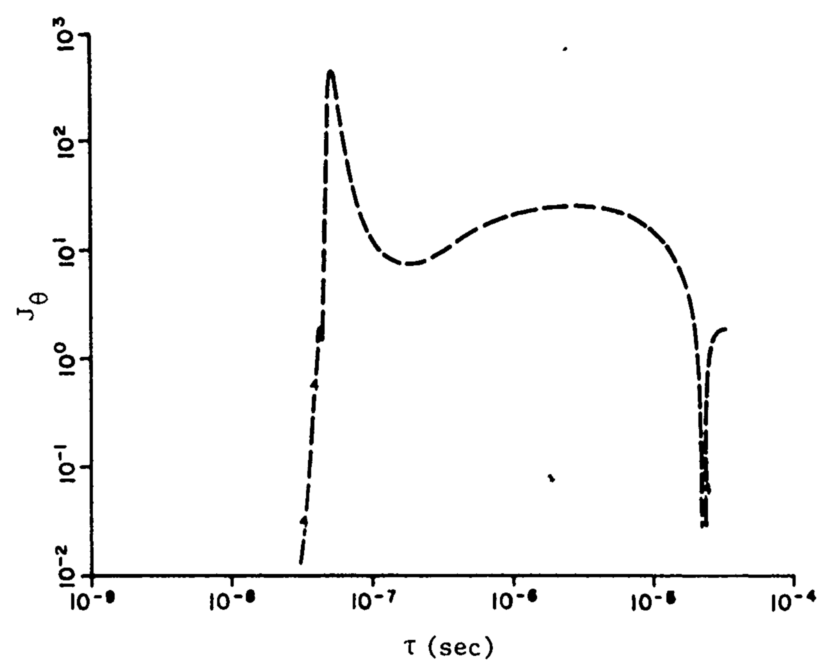

Fig. 14. Self-consistent theta current at 1000m, on the ground.

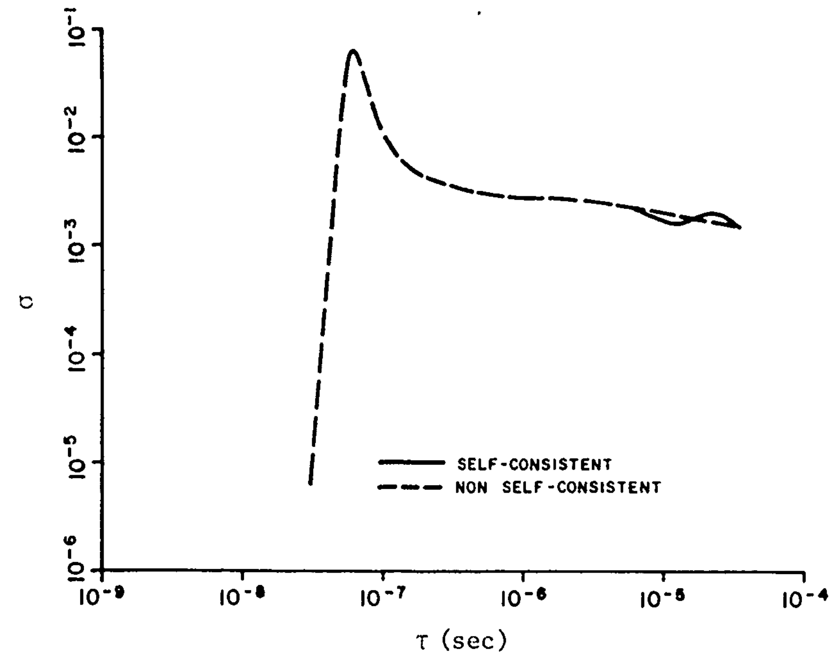

Fig. 15. Overlay, conductivities, 1000m.

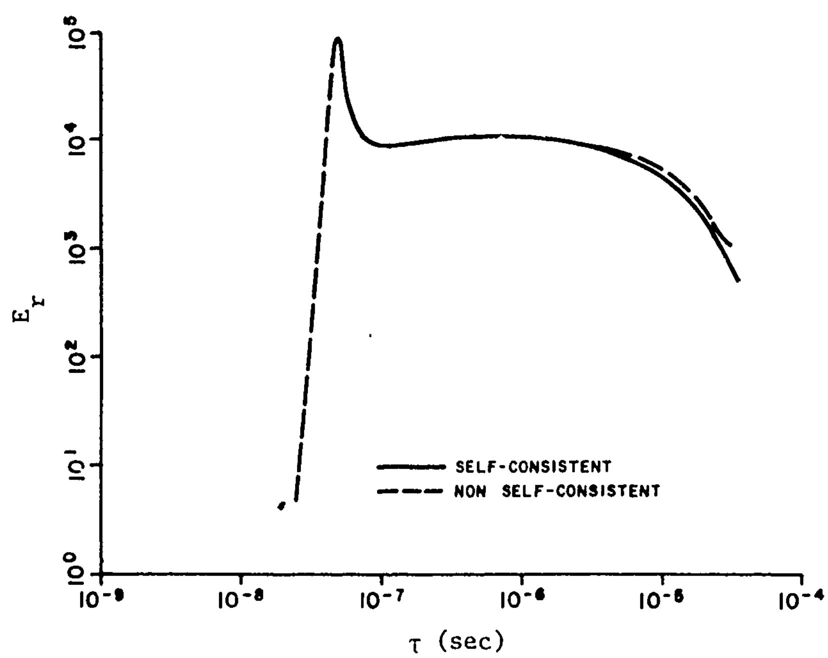

Fig. 16. Overlay, radial electric fields, 1000m.

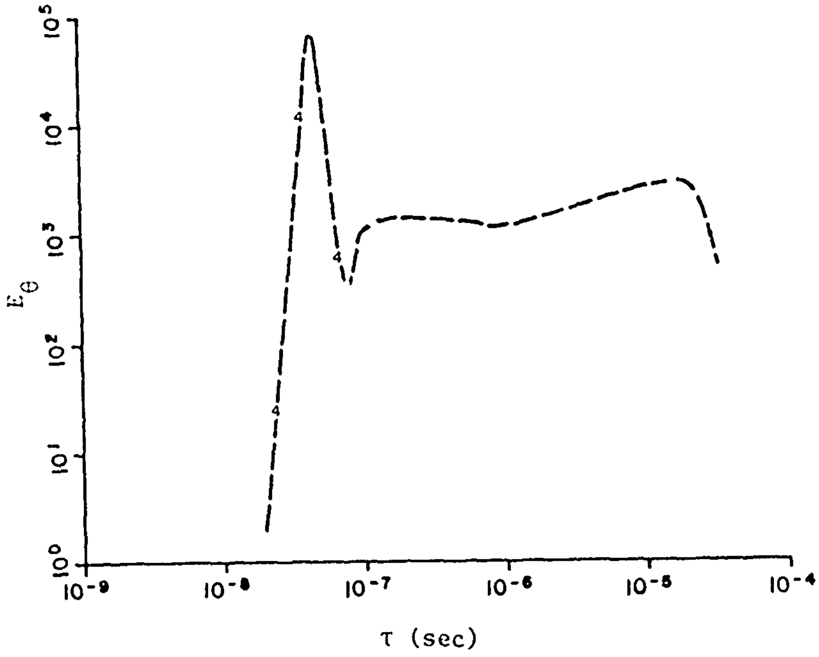

Fig. 17. Non-self-consistent theta electric field at 1000m, on the ground.

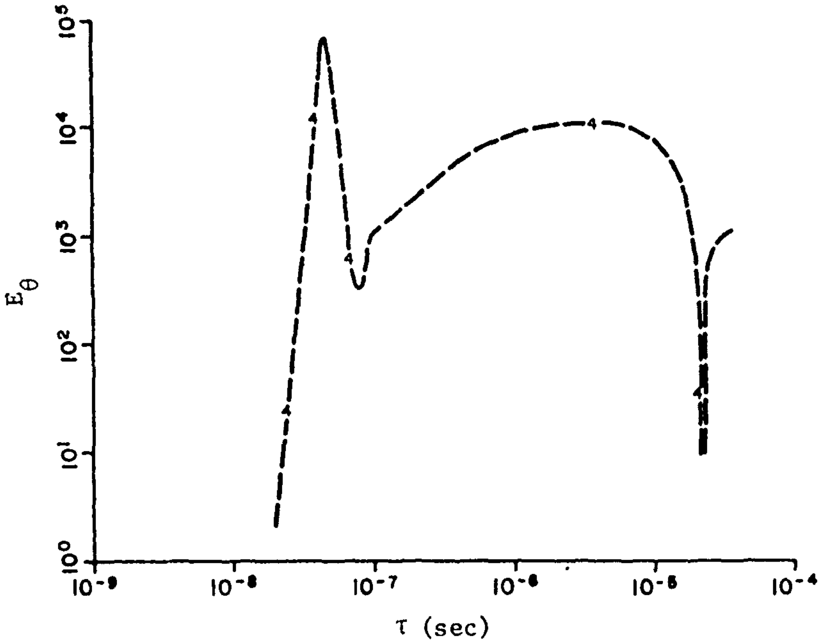

Fig. 18. Self-consistent theta electric field at 1000m, on the ground.

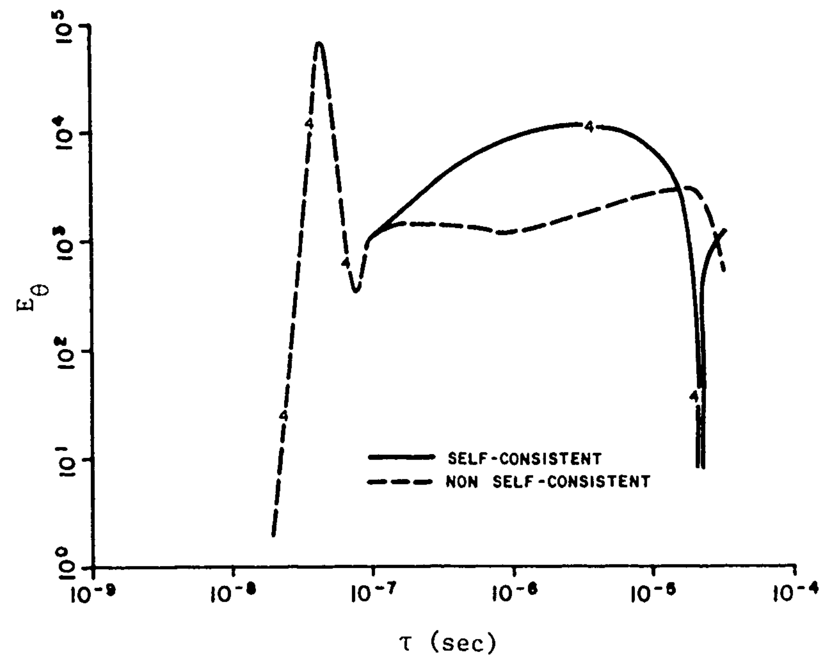

Fig. 19. Overlay, theta electric fields, 1000m.

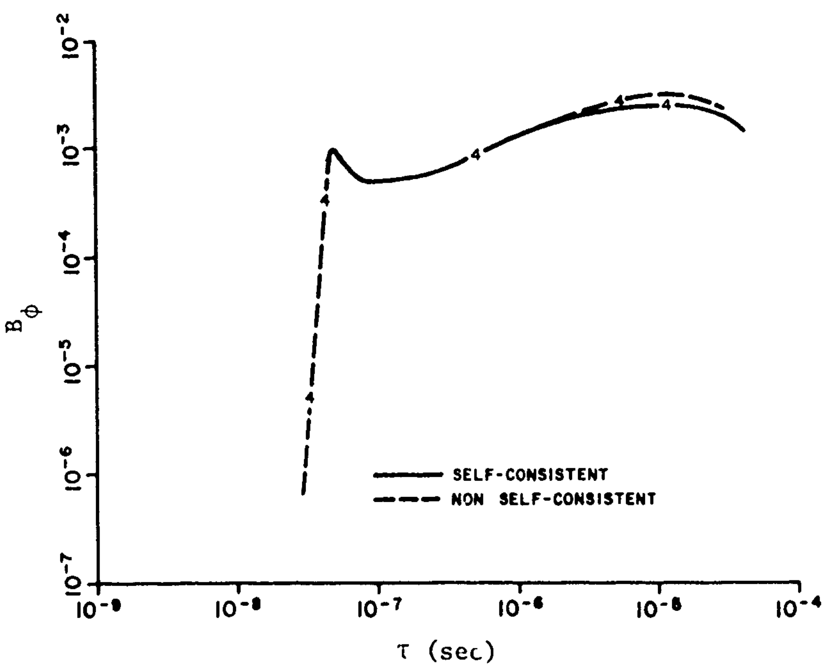

Fig. 20. Overlay, axial magnetic field, 1000m.

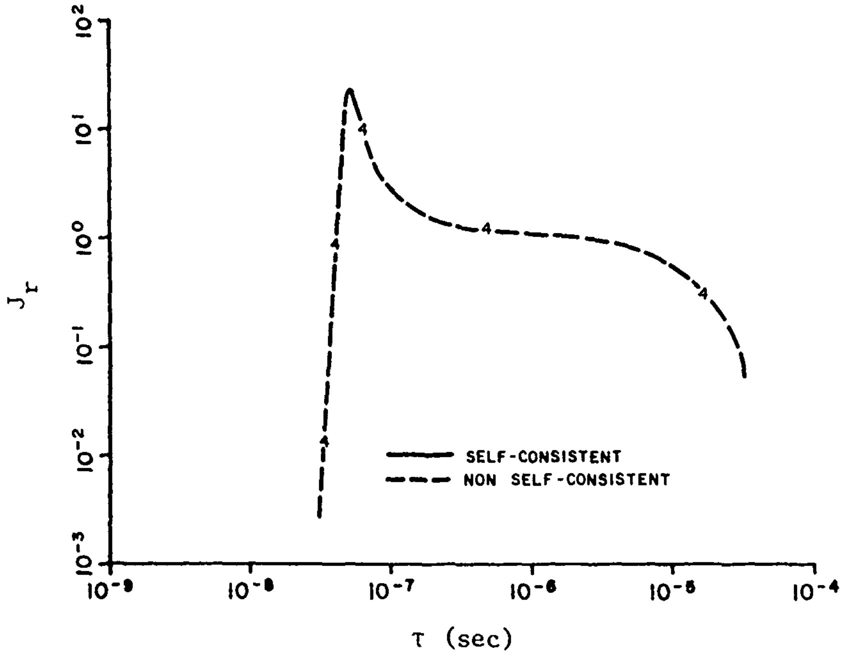

Fig. 21. Overlay, r dial currents, 2000m.

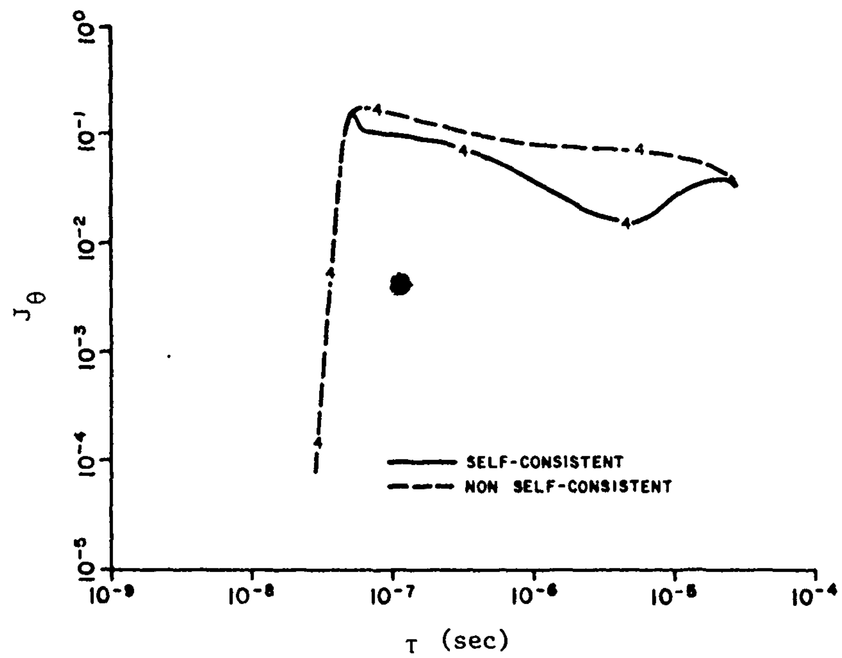

Fig. 22. Overlay, theta currents, 2000m.

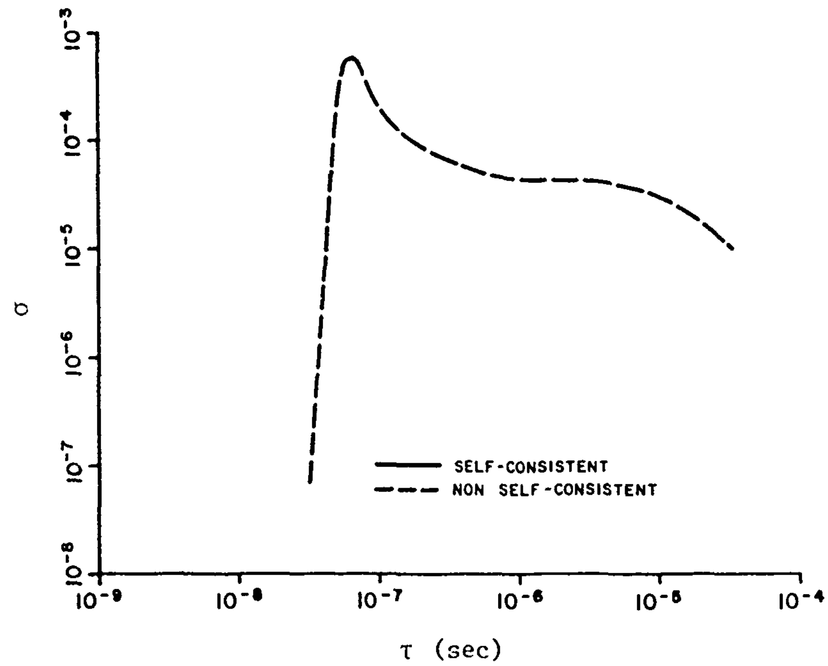

Fig. 23. Overlay, conductivity, 2000m.

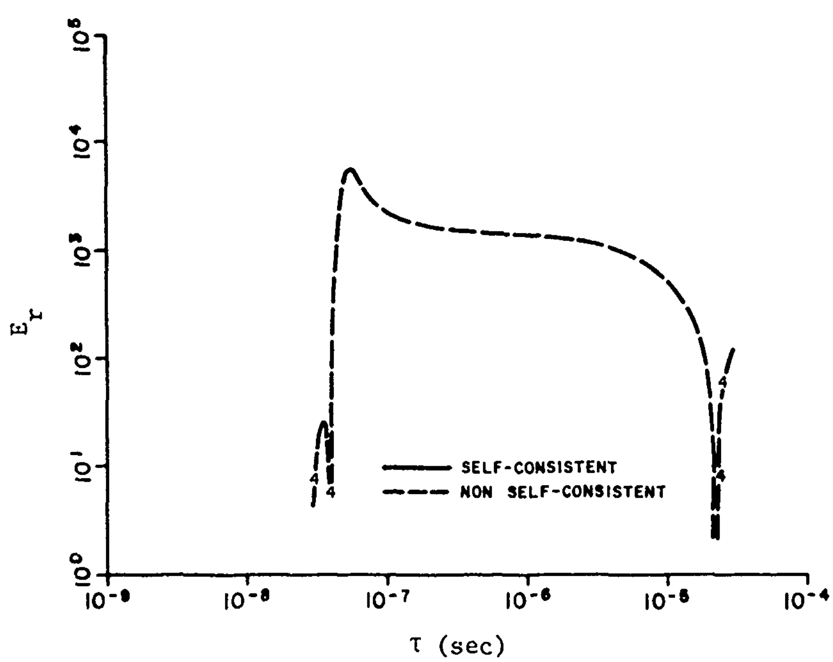

Fig. 24. Overlay, radial electric fields, 2000m.

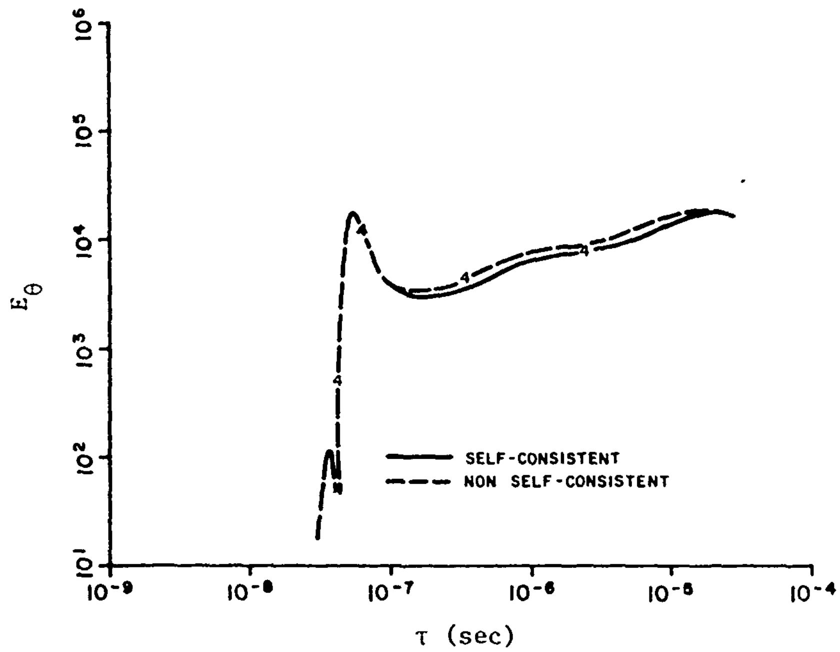

Fig. 25. Overlay, theta electric fields, 2000m.

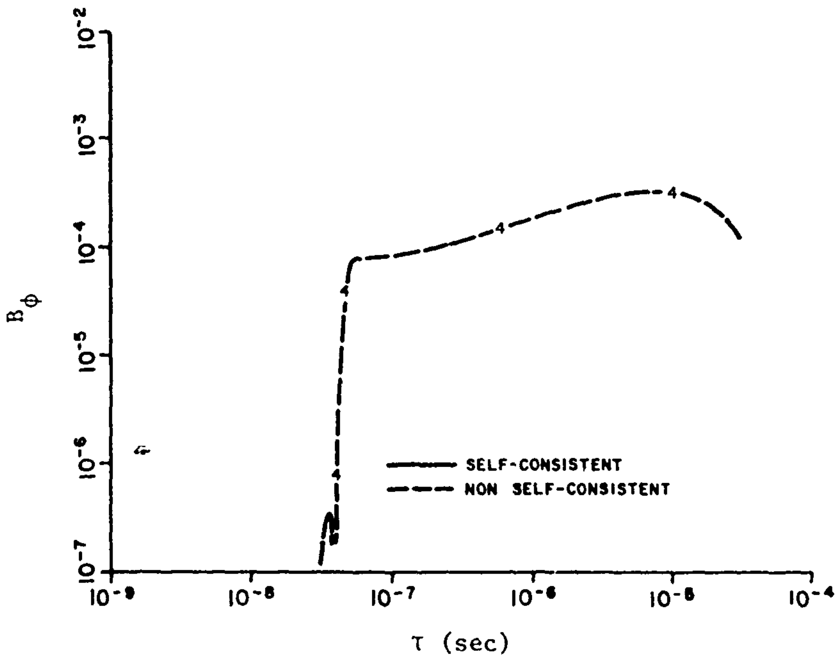

Fig. 26. Overlay, axial magnetic fields, 2000m.

SECTION V

RADIATION ENHANCED GROUND CONDUCTIVITY

In the past, SCX calculations have always assumed a uniform homogeneous ground with constant conductivity. However, in the real physical case, the deposition of radiation within the ground results in ionization which alters the conductivity from its ambient value. The time variation of the source and the nature of the deposition make the ground conductivity a function of both space and time. It is important to determine the effects of these possible variations on the EMP environments calculated with the SCX code.

To enhance calculational speed and efficiency, the coding in the SCX fields calculation has always implicitly assumed a constant ground conductivity. With the assumption of a variable conductivity, the differenced form of the radial equation in the ground becomes[3]

$$\left(\frac{1}{c_g^2} + \sigma_{ij}^{hk} \mu_g \frac{\delta t}{2}\right) E_{\rho_{ij}}^{hk} - \left(\frac{Z(\rho,z)}{2} - \frac{\delta t}{2\delta z_j}\right) B_{\phi_{ij}}^{k}$$

$$-\left(\frac{Z(\rho,z)}{2} + \frac{\delta t}{2\delta z_j}\right) B_{\phi_{ij-1}}^{k} = \left(\frac{1}{c_g^2} - \sigma_{ij}^{hk-1} \mu_g \frac{\delta t}{2}\right) E_{\rho_{ij}}^{hk-1}$$

$$-\left(\frac{Z(\rho,z)}{2} + \frac{\delta t}{2\delta z_j}\right) B_{\phi_{ij}}^{k-1} - \left(\frac{Z(\rho,z)}{2} - \frac{\delta t}{2\delta z_j}\right) B_{\phi_{ij-1}}^{k-1}$$

After the standard definition of constants, the following result is obtained

$$A1_j E_{\rho_{ij}}^{hk} - A21_j B_{\phi_{ij}}^{k} - A22_j B_{\phi_{ij-1}}^{k} = A3_j .$$

However, the following revised values of several constants must be used:

$$A1_j = \frac{1}{c_g^2} + \sigma_{ij}^{hk} \mu_g \frac{\delta t}{2}$$

$$A3_j = \left(\frac{1}{c_g^2} - \sigma_{ij}^{hk-1} \mu_g \frac{\delta t}{2}\right) E_{\rho_{ij}}^{hk-1}$$

$$-\left(\frac{Z(\rho,z)}{2} + \frac{\delta t}{2\delta z_j}\right) B_{\phi_{ij}}^{k-1} - \left(\frac{Z(\rho,z)}{2} - \frac{\delta t}{2\delta z_y}\right) B_{\phi_{ij-1}}^{k-1}$$

The other equation to be differenced which involves the conductivity is

$$R(\rho,z) \frac{\partial B_\phi}{\partial t} - \frac{1}{\rho} \frac{\partial}{\partial \rho}(\rho B_\phi) + \sigma \mu E_z \frac{1}{c_g^2} \frac{\partial E_z}{\partial \tau} = 0.$$

Assuming a variable conductivity, the following difference equation results

$$\left(R(\rho,z) - \frac{\rho_i}{\rho_i + \rho_{i-1}} \frac{\delta t}{\delta\rho}\right) B_{\phi_{ij}}^{k} + \left(\frac{1}{c_g^2} + \sigma_{ij}^{k}\mu_g \frac{\delta t}{2}\right) E_{z_{ij}}^{k}$$

$$= \left(\frac{1}{c_g^2} - \sigma_{ij}^{k-1}\ \mu_g \frac{\delta t}{2}\right) E_{z_{ij}}^{k-1} + \left(R(\rho,z) - \frac{\rho_i}{\rho_i + \rho_{i+1}} \frac{\delta t}{\delta\rho}\right) B_{\phi_{ij}}^{k-1}$$

$$- \left(\frac{\rho_{i-1}}{\rho_i + \rho_{i-1}} \frac{\delta t}{\delta\rho}\right) B_{\phi_{i-1j}}^{k} + \left(\frac{\rho_{i+1}}{\rho_i + \rho_{i-1}} \frac{\delta t}{\delta\rho}\right) B_{\phi_{i+1j}}^{k}$$

Definition of constants results in

$$A4_j B_{\phi_{ij}}^{k} + A5_j E_{z_{ij}}^{k} = A6_j \ ,$$

However, the following constants require new definition

$$A5_j = \frac{1}{c_g^2} + \sigma_{ij}^{k}\ \mu_g \frac{\delta t}{2} \quad (\neq A1_j \text{ for this case})$$

$$A6_j = \left(\frac{1}{c_g^2} - \sigma_{ij}^{k-1}\ \mu_g \frac{\delta t}{2}\right) E_{z_{ij}}^{k-1} + \left(R(\rho,z) - \frac{\rho_i}{\rho_i + \rho_{i+1}} \frac{\delta t}{\delta\rho}\right) B_{\phi_{ij}}^{k-1}$$

$$+ \left(\frac{\rho_{i+1}}{\rho_i + \rho_{i+1}} \frac{\delta t}{\delta\rho}\right) B_{\phi_{i+1j}}^{k-1} - \left(\frac{\rho_{i-1}}{\rho_i + \rho_{i-1}} \frac{\delta t}{\delta\rho}\right) B_{\phi_{i-1j}}^{k} \ .$$

When these changes are included in the field calculation subroutine of SCX, the effect of radiation enhanced ground conductivity may be examined.

Numerous models have been proposed to approximate the behavior of the ground conductivity with dose. To estimate the nature of the effect in SCX, it is convenient to use a simple model suggested by Graham and used by Jones[3]. In this approximation

$$\sigma_g(Q,z) = \sigma_g(\text{constant}) + \frac{1 \times 10^{-14}}{8.081 \times 10^{10}} \frac{34}{10^6} Qe^{20z}$$

where

Q is the ionization rate at the ground

$8.081 \times 10^{10} \frac{\text{mev}}{\text{m}^3} = 1$ rad air

z is the depth in meters (a negative number), and

σ_g(constant) is the normal ground conductivity.

For a source on the ground, as is the case in SCX, the deposition beneath the surface is rather small for ranges greater than a few hundred meters. A typical value for the ground conductivity in SCX calculations is 0.01 mhos/meter. Figure 1 shows the radiation enhanced conductivity as a function of time 5 cm below the surface at a range of 250 meters in a typical SCX run. It can be seen that the values change by at most about 50% near the peak. Near the prompt peak, values of the transverse electric field on the

ground decrease by up to 30% for an observer at 250 meters. By 500 meters, the decrease is more like 5%. For the farther observers, the time histories compare within a line width. Thus, except for very close in observers there is little or no effect of enhanced conductivity on SCX results. This was the expected result for a ground burst due to the very small deposition in the ground. For a near surface case where the deposition can be orders of magnitude greater for down range observers, significant results would be expected.

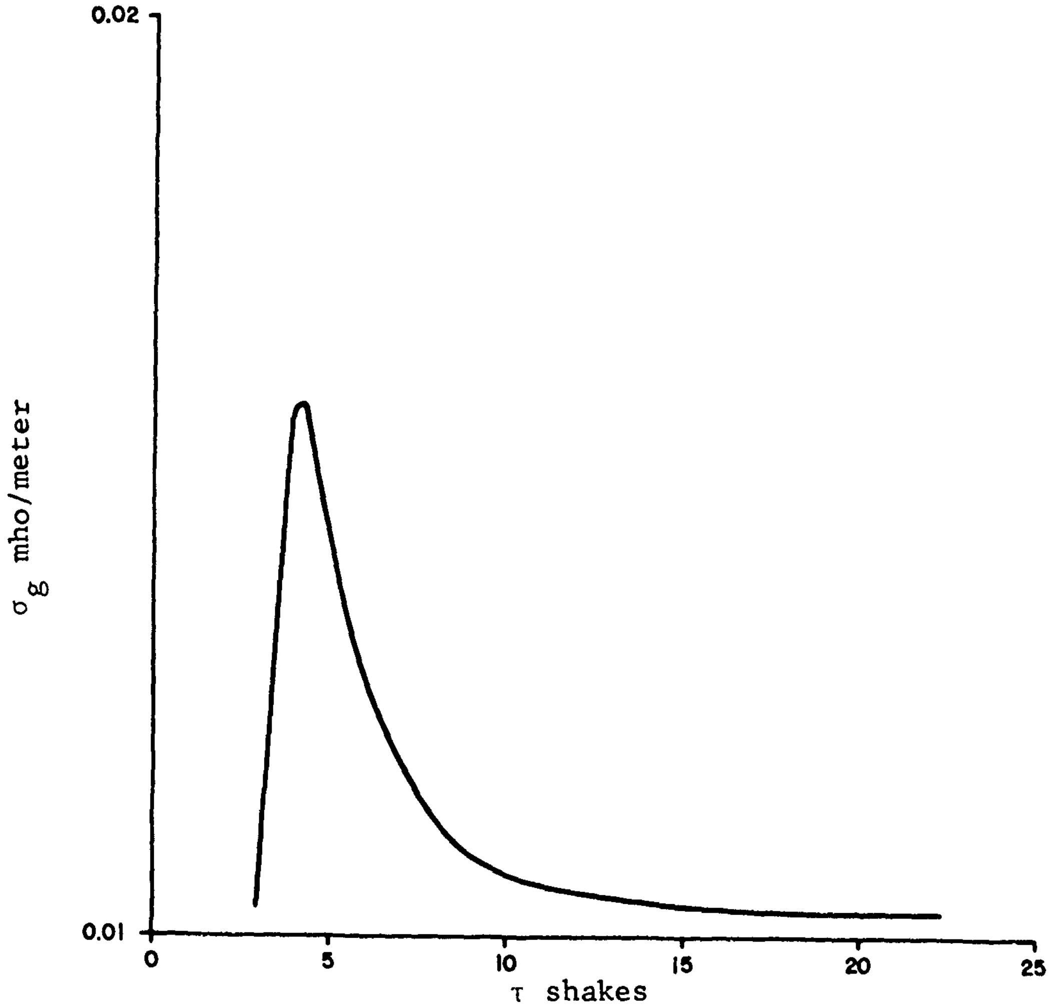

Figure 27. Radiation Enhanced Ground Conductivity vs. Time for Range of 250m and Depth of .05m.

REFERENCES

1. Dalich, S. J., "SCX: A Two-Dimensional Ground Burst EMP Code," SAI-73-501-AQ, June 1973.

2. Longley, H. J., "Compton Current in Presence of Fields for LEMP 1," EMP Theoretical Note 77, Vol. 2-4.

3. Jones, C. W., "EMP Comparisons of Photon Transport in the Vicinity of a Material Interface with Photon Transport in a Homogeneous Atmosphere," DC-TN-2153-2, 1972.

DISTRIBUTION LIST

DEPARTMENT OF DEFENSE

Director
Armed Forces Radiobiology Research Institute
Defense Nuclear Agency
ATTN: Technical Library
ATTN: Robert E. Carter

Assistant to the Secretary of Defense
Atomic Energy
ATTN: Document Control

Director
Defense Advanced Research Project Agency
ATTN: Technical Library
ATTN: AD/E&PS, George H. Halmeier
ATTN: NMR

Director
Defense Civil Preparedness Agency
ATTN: TS AED
ATTN: RE EO
ATTN: Technical Library

Defense Communication Engineer Center
ATTN: Code R-720, C. Stansberry
ATTN: Code R-410, James W. McLean
ATTN: Code R-400
ATTN: Code R-124C, Technical Library

Director
Defense Communications Agency
ATTN: Code 950
ATTN: Technical Library
ATTN: Code 430
ATTN: Code 930, Franklin D. Moore
ATTN: Code 930, Monte I. Burgett, Jr.

Defense Documentation Center
12 cy ATTN: TC

Commander
Defense Electronic Supply Center
ATTN: ECS
ATTN: EQ
ATTN: Technical Library

Director
Defense Intelligence Agency
ATTN: DI-7D, Edward O'Farrell
ATTN: DI-7D
ATTN: DI-3
ATTN: Technical Library

Director
Defense Nuclear Agency
ATTN: STSI, Archives
ATTN: RAAE
ATTN: DDST
ATTN: RATN
ATTN: RAEV
ATTN: STVL
ATTN: PPSR
2 cy ATTN: SPSS
2 cy ATTN: STAP
5 cy ATTN: SPAS, D. Kohler
2 cy ATTN: STTL, Technical Library

DEPARTMENT OF DEFENSE (Continued)

Headquarters
European Command
ATTN: Technical Library

Commander
Field Command
Defense Nuclear Agency
ATTN: FCPR

Director
Interservice Nuclear Weapons School
ATTN: Document Control
ATTN: Technical Library

Director
Joint Strategic Target Planning Staff, JCS
ATTN: JSAS
ATTN: JLTW-2
ATTN: STINFO Library

Chief
Livermore Division, Field Command, DNA
ATTN: Document Control for L-395
ATTN: FCPRL

National Communications System
ATTN: NCS-TS, Charles D. Bodson

DDR&E
ATTN: Asst. Dir., Strat. Wpns.

Director
National Security Agency
ATTN: Technical Library
ATTN: TDL
ATTN: Orland O. Van Gunten, R-425

OJCS/J-6
ATTN: J-6, ESD-2

Director
Telecommunications & Command & Control System
ATTN: AD/ODTACCS
ATTN: Dep. Asst., Sec. Sys.

Commander-in-Chief
U.S. European Command, JCS
ATTN: Technical Library

Weapons Systems Evaluation Group
ATTN: Document Control

DEPARTMENT OF THE ARMY

Asst. Chief of Staff for Intelligence
ATTN: DAMA-TAS, Jack T. Blackwell

Commander
Ballistic Defense System Command
ATTN: Technical Library
ATTN: BDMSC-TEN, Noah J. Hurst

Director
Ballistic Missile Defense Advanced Technical Center
ATTN: Technical Library

PRECEDING PAGE BLANK-NOT FILMED

DEPARTMENT OF THE ARMY (Continued)

Chief of Research, Development & Acquisition
Department of the Army
ATTN: DAMA-CSM-N, LTC E. V. DeBoeser, Jr.

Commander
Harry Diamond Laboratories
ATTN: AMXDO-TI, Technical Library
ATTN: AMXDO-EM, Ron Bostak
ATTN: AMXDO-EM, John Bombardt
ATTN: AMXDO-RB, Joseph R. Miletta
ATTN: AMXDO-TR, Edward E. Conrad
ATTN: AMXDO-EM, William T. Wyatt, Jr.
ATTN: AMXDO-NP, Francis N. Wimenitz
ATTN: AMXDO-RBI, John A. Rosado
ATTN: AMXDO-RB, Robert E. McCoskey
ATTN: AMXDO-RCC, John E. Thompkins

Commander
Picatinny Arsenal
ATTN: SMUPA-ND-W
ATTN: SARPA-ND-C-E, Amina Nordio
ATTN: SMUPA-TN, Burton V. Franks
ATTN: Paul Harris
ATTN: Technical Library
ATTN: SMUPA-ND-D-C-2
ATTN: SARPA-TS-I-E, Abraham Grinoch

Commander
Redstone Scientific Information Center
4 cy ATTN: AMSMI-RBD, Clara T. Rogers

Commander
U.S. Army Armor Center
ATTN: ATSAR-CD-MS
ATTN: Technical Library

Director
U.S. Army Ballistic Research Laboratories
ATTN: AMXBR-AM, W. R. VanAntwerp
ATTN: AMXBR-VL, John W. Kinch
ATTN: AMXRD-BVL, David L. Rigotti
ATTN: AMXBR-X, Julius J. Meszaros
ATTN: Technical Library, Edward Baicy

U.S. Army Communications Command
C-E Services Division
ATTN: CEEO-7, Wesley T. Heath, Jr.

Commander
U.S. Army Communications Command
ATTN: Technical Library

Commander
U.S. Army Communications Command
ATTN: ACCM-TD-A, Library

Chief
U.S. Army Communications System Agency
ATTN: SCCM-AD-SV, Library

Commander
U.S. Army Computer Systems Command
ATTN: Technical Library

Commander Officer
U.S. Army Electronics Command
ATTN: Technical Library

DEPARTMENT OF THE ARMY (Continued)

Commander
U.S. Army Electronics Command
ATTN: AMSEL-NL-D
ATTN: AMSEL-CE, T. Preiffer
ATTN: AMSEL-CT-HDK, Abraham E. Cohen
ATTN: AMSEL-GG-TD, W. R. Werk
ATTN: AMSEL-WL-D
ATTN: AMSEL-TL-MD, Gerhart K. Gaule
ATTN: AMSEL-TL-ME, M. W. Pomerantz
ATTN: AMSEL-TL-IR, Robert A. Freiberg
ATTN: AMSEL-PL-ENV, Hans A. Bomke

Commander
U.S. Army Electronics Proving Ground
ATTN: STEEP-MT-M, Gerald W. Durbin

Division Engineer
U.S. Army Engr. Dist. Missouri River
ATTN: MRDED-MC, Floyd L. Hazlett

Commander-in-Chief
U.S. Army Europe & Seventh Army
ATTN: Technical Library

Commandant
U.S. Army Field Artillery School
ATTN: ATSFA-CTD-ME, Harley Moberg
ATTN: Technical Library

Commander
U.S. Army Mat. & Mechanics Research Center
ATTN: AMXMR-HH, John F. Dignam
ATTN: Technical Library

Director
U.S. Army Material Sys. Analysis Agency
ATTN: AMXSY-CC, Donald R. Barthel
ATTN: Technical Library

Commander
U.S. Army Materiel Command
ATTN: AMCRD-WN-RE, John F. Corrigan
ATTN: Technical Library

Commander
U.S. Army Missile Command
ATTN: AMSMI-RGD, Vic Ruwe
ATTN: AMCPM-LCEX, Howard H. Henriksen
ATTN: AMCPM-PE-EG, William B. Johnson
ATTN: AMSMI-RGP, Hugh Green
ATTN: AMCPM-PE-EA, Wallace O. Wagner
ATTN: Technical Library

Commander
U.S. Army Mobility Equip. R&D Center
ATTN: STSFB-MW, John W. Bond, Jr.
ATTN: Technical Library

Commander
U.S. Army Nuclear Agency
ATTN: ATCN-W, LTC Leonard A. Sluga
ATTN: Technical Library

Commander
U.S. Army Security Agency
ATTN: IARD-T, Robert H. Burkhardt
ATTN: Technical Library

DEPARTMENT OF THE ARMY (Continued)

Commandant
U.S. Army Southeastern Signal School
ATTN: Technical Library
ATTN: ATSO-CTD-CS, CPT G. M. Alexander

Project Manager
U.S. Army Tactical Data Systems, AMC
ATTN: Technical Library

Commander
U.S. Army Tank Automotive Command
ATTN: Technical Library
ATTN: AMCPM-GCM-SW, Lyle A. Wolcott

Commander
U.S. Army Test & Evaluation Command
ATTN: AMSTE-NB, Russell R. Galasso
ATTN: AMSTE-EL, Richard I. Kolchin
ATTN: Technical Library

Commander
U.S. Army Training & Doctrine Command
ATTN: Technical Library
ATTN: ATORI-OP-SD

Commander
White Sands Missile Range
ATTN STEWS-TE-NT, Marvin P. Squires
ATTN. Technical Library

DEPARTMENT OF THE NAVY

Chief of Naval Operations
Navy Department
ATTN: Code 604C3, Robert Piacesi

Chief of Naval Research
Navy Department
ATTN: Code 464. Thomas P. Quinn
ATTN: Code 127
ATTN: Technical Library

Officer-in-Charge
Civil Engineering Laboratory
ATTN: Technical Library
ATTN: Code L-31

Commander
Naval Air Systems Command
Headquarters
ATTN: Technical Library
ATTN: AIR-350F, LCDR Hugo Hart

Commanding Officer
Naval Ammunition Depot
ATTN: Technical Library
ATTN: Code 7024, James Ramsey

Commander
Naval Electronic Systems Command
Naval Electronic Systems Command Headquarters
ATTN: PME 117-T
ATTN: PME 117-215A, Gunter Brunhart
ATTN: PME 117-21
ATTN: Technical Library

DEPARTMENT OF THE NAVY (Continued)

Commander
Naval Electronics Laboratory Center
ATTN: Code 2200, Verne E. Hildebrand
ATTN: Code 3100, E. E. McCown
ATTN: Code 2100, S. W. Lichtman
ATTN. Technical Library

Commanding Officer
Naval Intelligence Support Center
ATTN: NISC-45
ATTN: Technical Library

Superintendent
Naval Postgraduate School
ATTN: Code 2124, Technical Reports Librarian

Director
Naval Research Laboratory
ATTN: Code 2627, Doris R. Folen
ATTN: Code 2027, Technical Library
ATTN: Code 4004, Emanual L. Brancato
ATTN: Code 6631, James C. Ritter
ATTN: Code 7706, Jay P. Boris
ATTN: Code 7701, Jack D. Brown
ATTN: Code 7770, Leslie S. Levine
ATTN: Code 461, R. Gracen Joiner

Commander
Naval Sea Systems Command
Navy Department
ATTN: SEA-9931, Riley B. Lane

Commander
Naval Ship Engineering Center
ATTN: Technical Library
ATTN: Code 6174D2, Edward F. Duffy

Commander
Naval Surface Weapons Center
ATTN: Code 1224, Navy Nuc. Prgms. Off.
ATTN: Code 431, John H. Malloy
ATTN: Code WR-43
ATTN: Code 431, Edwin R. Rathburn
6 cy ATTN: Code 730, Technical Library

Commander
Naval Surface Weapons Center
ATTN: Technical Library

Commander
Naval Telecommunications Command
ATTN: Technical Library

Commander
Naval Weapons Center
ATTN: Code 533, Technical Library

Commanding Officer
Naval Weapons Evaluation Facility
ATTN: Lawrence R. Oliver
ATTN: Code ATG, Mr. Stanley
ATTN: ADS

DEPARTMENT OF THE NAVY (Continued)

Commanding Officer
Navy Astronautics Group
ATTN: Technical Library

Commanding Officer
Nuclear Weapons Training Center, Pacific
ATTN: Code 50

Director
Strategic Systems Project Office
Navy Department
ATTN: NSP-43, Technical Library
ATTN: NSP-2431, Gerald W. Hoskins
ATTN: NSP-230, David Gold
ATTN: SP-2701, John W. Pitsenberger

Commander
U.S. Naval Coastal Systems Laboratory
ATTN: Technical Library

Commander-in-Chief
U.S. Pacific Fleet
ATTN: Document Control

DEPARTMENT OF THE AIR FORCE

Commander
ADC/DE
ATTN: DEEDS, Joseph C. Brannan
ATTN: DDEEN

Commander
ADC/XP
ATTN: XPQDQ, Maj G. Kuch
ATTN: XPDQ

Commander
Aeronautical Systems Division, AFSC
ATTN: Technical Library

AF Armament Laboratory, AFSC
ATTN: DLOSL, Library

AF Cambridge Research Laboratories, AFSC
ATTN: J. Emery Cormier

AF Weapons Laboratory, AFSC
ATTN: ELP, William Page
ATTN: ELP, Carl E. Baum
ATTN: HO, Dr. Minge
ATTN: DYV, Maj Mitchell
ATTN: DYV, Capt Scammon
ATTN: DYV, Lt Mac Farlane
ATTN: DYX, Donald C. Wunsch
ATTN: EL, John Darrah
ATTN: ELA, J. P. Castillo
ATTN: SAT
ATTN: SAB
ATTN: EL
ATTN: EL, Library
ATTN: DY
ATTN: DYV, Maj Stuber
ATTN: DYV, Dr. Place
ATTN: DYV, Mr. Bick
2 cy ATTN: SUL

AFISC
ATTN: PQAL

DEPARTMENT OF THE AIR FORCE (Continued)

AFTAC
ATTN: Technical Library
ATTN: TAP

Air Force Avionics Laboratory, AFSC
ATTN: Technical Library

AUL
ATTN: LDE

AFML
ATTN: Technical Library

Dir. Nuc. Safety
ATTN: SN

Headquarters
Air Force Systems Command
ATTN: Technical Library

Commander
Air University
ATTN: AUL/LSE-70-250

Headquarters
Electronic Systems Division, AFSC
ATTN: Technical Library
ATTN: YWEI
ATTN: XRT, Lt Col John M. Jasinski
ATTN: YSEV, Lt Col David C. Sparks

Commander
Foreign Technology Technology Division, AFSC
ATTN: TD-BTA, Library
ATTN: ETET, Capt Richard C. Husemann

HQUSAF/RD
ATTN: RDQPN

Commander
Ogden Air Logistics Center
ATTN: MMEWM, Robert Joffs
ATTN: Technical Library

Commander
Rome Air Development Center, AFSC
ATTN: EMTLD, Document Library

Commander
Sacramento Air Logistics Center
ATTN: Technical Library

SAMSO/MN
ATTN: MNNH, Capt Michael V. Bell
ATTN: MNNH, Capt B. Stewart
ATTN: MNNR

SAMSO/RS
ATTN: RSSE
ATTN: Technical Library

SAMSO/SK
ATTN: SKF, Peter H. Stadler

SAMSO/YD
ATTN: YDD, Maj Marion F. Schneider

USAF
SCLO
ATTN: Maj J. H. Pierson, Chief, LO

DEPARTMENT OF THE AIR FORCE (Continued)

Commander in Chief
Strategic Air Command
ATTN: DEF, Frank N. Bousha
ATTN: NRI-STINFO Library
ATTN: XPFS, Maj Brian G. Stephan

544th IES
ATTN: RDPO, Lt Alan B. Merrill

ENERGY RESEARCH & DEVELOPMENT ADMINISTRATION

Division of Military Application
U.S. Energy Research & Development Administration
ATTN: Document Control for Class. Tech. Lib.

EG&G, Inc.
Los Alamos Division
ATTN: L. Detch
ATTN: Technical Library

University of California
Lawrence Berkeley Laboratory
ATTN: Library, Bldg. 50, Rm. 134
ATTN: Kenneth M. Watson

University of California
Lawrence Livermore Laboratory
ATTN: William J. Hogan, L-531
ATTN: Frederick R. Kovar, L-94
ATTN: Hans Kruger, L-96
ATTN: Leland C. Loquist
ATTN: Technical Information Department, L-3
ATTN: Louis F. Wouters, L-24
ATTN: Donald J. Meeker, L-153
ATTN: Robert A. Anderson, L-156
ATTN: Terry R. Donich

Los Alamos Scientific Laboratory
ATTN: Document Control for John S. Malik
ATTN: Document Control for J. Arthur Freed
ATTN: Document Control for Richard L. Wakefield
ATTN: Document Control for Reports Library
ATTN: Document Control for J-8, R. E. Dartridge

Sandia Laboratories
Livermore Laboratory
ATTN: Document Control for Technical Library

Sandia Laboratories
ATTN: Document Control for Charles N. Vittitoe
ATTN: Document Control for Elmer F. Hartman
ATTN: Document Control for 5245, T. H. Martin
ATTN: Document Control for Org. 9353, R. L. Parker
ATTN: Document Control for Gerald W. Barr, 1114
ATTN: Document Control for Org. 3141, Sandia Rpt. Coll.

U.S. Energy Research & Development Administration
Albuquerque Operations Office
ATTN: Document Control for WSSB
ATTN: Document Control for Technical Library

Union Carbide Corporation
Holifield National Laboratory
ATTN: Paul R. Barnes
ATTN: Document Control for Technical Library

OTHER GOVERNMENT AGENCIES

Central Intelligence Agency
ATTN: RD/SI for William A. Decker
ATTN: RD/SI for Technical Library

Administrator
Defense Electric Power Administration
Department of the Interior
ATTN: Document Control

Department of Commerce
National Bureau of Standards
ATTN: Technical Library

Department of Commerce
National Oceanic & Atmospheric Administration
ATTN: Classified Document Library

Federal Aviation Administration
Headquarters Security Branch, ASE-210
ATTN: ARD-350
ATTN: Fredrick S. Sakate, ARD-350

NASA
ATTN: Technical Library
ATTN: Code Res. Guid. Con. & Info. Sys.

NASA
Lewis Research Center
ATTN: Library

DEPARTMENT OF DEFENSE CONTRACTORS

Aerojet Electro-Systems Co. Div.
Aerojet-General Corporation
ATTN: Technical Library
ATTN: Thomas D. Hanscome

Aeronutronic Ford Corporation
Aerospace & Communications Ops.
ATTN: Ken C. Attinger
ATTN: E. R. Poncelet, Jr.
ATTN: L. H. Linder
ATTN: Technical Information Section

Aeronutronic Ford Corporation
Western Development Laboratories Division
ATTN: Samuel R. Crawford, MS 531
ATTN: J. T. Mattingly, MS X-22
ATTN: Library

Aerospace Corporation
ATTN: Bal Krishan
ATTN: Melvin J. Bernstein
ATTN: S. P. Bower
ATTN: Julian Reinheimer
ATTN: Irving M. Garfunkel
ATTN: Dr. B. Barry
ATTN: Norman D. Stockwell
ATTN: Library

Avco Research & Systems Group
ATTN: Research Library A830, Rm. 7201
ATTN: W. Broding

Battelle Memorial Institute
ATTN: Technical Library
ATTN: David A. Dingee
ATTN: Dr. L. E. Hulbert

The BDM Corporation
ATTN: Technical Library

The BDM Corporation
ATTN: Technical Library
ATTN: Robert B. Buchanan
ATTN: T. H. Neighbors

Bell Aerospace Company
Division of Textron, Inc.
ATTN: Carl B. Schoch, Wpns. Effects Grp.
ATTN: Martin A. Henry
ATTN: Technical Library

The Bendix Corporation
Communication Division
ATTN: Document Control

The Bendix Corporation
Research Laboratories Division
ATTN: Technical Library
ATTN: Donald J. Niehaus, Mgr. Prgm. Dev.

The Bendix Corporation
Navigation & Control Division
ATTN: Technical Library

The Boeing Company
ATTN: David Kemle
ATTN: David L. Dye, MS 87-75
ATTN: Howard W. Wicklein, MS 17-11
ATTN: D. E. Isbell
ATTN: Dr. B. Lampriere
ATTN: Aerospace Library

Booz-Allen & Hamilton, Inc.
ATTN: Raymond J. Chrisner
ATTN: Technical Library

Brown Engineering Company, Inc.
ATTN. David L. Lambert, MS 18
ATTN: John M. McSwain, MS 18
ATTN: Technical Library, P. Shelton, MS 12

Burroughs Corporation
Federal & Special Systems Group
ATTN: Angelo J. Mauriello
ATTN: Technical Library

Calspan Corporation
ATTN: Technical Library

Charles Stark Draper Laboratory, Inc.
ATTN: Technical Library
ATTN: Kenneth Fertig

Cincinnati Electronics Corporation
ATTN: Technical Library

Computer Sciences Corporation
ATTN: Technical Library

Computer Sciences Corporation
ATTN: Alvin T. Schiff

Cutler-Hammer, Inc.
AIL Division
ATTN: Anne Anthony, Central Technical Files

DEPARTMENT OF DEFENSE CONTRACTORS (Continued)

University of Denver
Colorado Seminary
ATTN: Security Officer for Ron W. Buchanon
ATTN: Security Officer for Technical Library
ATTN: Security Officer for Fred P. Venditti

The Dikewood Corporation
ATTN: L. Wayne Davis
ATTN: Technical Library

E-Systems, Inc.
Greenville Division
ATTN: Library 8-50100

Effects Technology, Inc.
ATTN: Edward John Steele
ATTN: B. Wengler
ATTN: Technical Library

EG&G, Inc.
Albuquerque Division
ATTN: Technical Library

ESL, Inc.
ATTN: Technical Library
ATTN: William Metzer

Experimental & Mathematical Physics Consultants
ATTN: Thomas M. Jordan

Fairchild Camera & Instrument Corporation
ATTN: Security Department for Technical Library

Fairchild Industries, Inc.
Sherman Fairchild Technology Center
ATTN: Leonard J. Schreiber
ATTN: Technical Library

The Franklin Institute
ATTN: Ramie H. Thompson
ATTN: Technical Library

Garrett Corporation
ATTN: Technical Library

General Dynamics Corporation
Pomona Operation
ATTN: Technical Library

General Dynamics Corporation
Electronics Division
ATTN: Technical Library

General Electric Company
Space Division
ATTN: Technical Information Center
ATTN: Larry I. Chasen
ATTN: Joseph C. Peden, CCF-8301
ATTN: Dante M. Tasca
ATTN: James P. Spratt
ATTN: Daniel Edelman
ATTN: J. Hannabeck

General Electric Company
Re-Entry & Environmental Systems Division
ATTN: John W. Palchefsky, Jr.
ATTN: Technical Library

DEPARTMENT OF DEFENSE CONTRACTORS (Continued)

General Electric Company
Ordnance Systems
ATTN: Joseph J. Reidl

General Electric Company
TEMPO-Center for Advanced Studies
ATTN: Royden R. Rutherford
ATTN: DASIAC

General Electric Company
ATTN: Richard C. Fries, CSP 6-7
ATTN: Technical Library

General Electric Company
Aircraft Engine Group
ATTN: John A. Ellerhorst, E-2
ATTN: Technical Library

General Electric Company
Aerospace Electronics Systems
ATTN: George Francis, Drop 233
ATTN: Charles M. Hewison, Drop 624
ATTN: Technical Library

General Electric Company
ATTN: Technical Library

General Research Corporation
ATTN: John Ise, Jr.
ATTN: Robert D. Hill
ATTN: Technical Information Office

Grumman Aerospace Corporation
ATTN: Jerry Rogers, Department 533
ATTN: Technical Library

GTE Sylvania, Inc.
Electronics Systems Group-Eastern Division
ATTN: James A. Waldon
ATTN: Charles A. Thornhill, Librarian
ATTN: Leonard L. Blaisdell

GTE Sylvania, Inc.
ATTN: Herbert A. Ullman
ATTN: Mario A. Nurefora, H & V Group
ATTN: S. E. Perlman, A.S.M. Department
ATTN: David P. Flood
ATTN: Emil P. Motchok, Comm. Syst.

Harris Corporation
Harris Semiconductor Division
ATTN: Wayne E. Abare, MS 16-111
ATTN: Carl F. Davis, MS 17-220
ATTN: T. L. Clark, MS 4040
ATTN: Technical Library

Hazeltine Corporation
ATTN: M. Waite, Technical Information Center

Hercules, Incorporated
ATTN: Technical Library
ATTN: R. Woodruff, 100K-26-W

Honeywell Incorporated
Government & Aeronautical Products Division
ATTN: Ronald R. Johnson, A-1622
ATTN: Technical Library

DEPARTMENT OF DEFENSE CONTRACTORS (Continued)

Honeywell Incorporated
Aerospace Division
ATTN: Stacey H. Graff, MS 725-J
ATTN: Technical Library

Honeywell Incorporated
Radiation Center
ATTN: Technical Library

Hughes Aircraft Company
ATTN: Billy W. Campbell, MS 6-E-110
ATTN: Technical Library

Hughes Aircraft Company
Ground Systems Group
ATTN: Library, MS C-222

Hughes Aircraft Company
Space Systems Division
ATTN: Edward C. Smith, MS A-620
ATTN: William W. Scott, MS A-1080
ATTN: Technical Library

IBM Corporation
ATTN: Frank Frankovsky
ATTN: Technical Library

IIT Research Institute
ATTN: ACOAT
ATTN: Technical Library

IIT Research Institute
ATTN: Irving N. Mindel
ATTN: Technical Library

Institute for Defense Analyses
ATTN: IDA Librarian, Ruth S. Smith

Intelcom Rad Tech
ATTN: R. L. Mertz
ATTN: Ralph H. Stahl
ATTN: Technical Library

International Telephone & Telegraph Corporation
ATTN: J. Gulack, Def. Sp. Grp.
ATTN: Technical Library

Ion Physics Corporation
ATTN: Robert D. Evans
ATTN: H. Milde
ATTN: B. Evans
ATTN: Technical Library

Johns Hopkins University
Applied Physics Laboratory
ATTN: Technical Library

Litton Systems, Inc.
Data Systems Division
ATTN: Technical Library

Litton Systems, Inc.
Guidance & Control Systems Division
ATTN: John P. Retzler
ATTN: Val J. Ashby, MS 67
ATTN: Technical Library

Ktech Corporation
ATTN: Dr. D. Keller

DEPARTMENT OF DEFENSE CONTRACTORS (Continued)

Kaman Sciences Corporation
ATTN: W. Foster Rich
ATTN: Walter E. Ware
ATTN: John R. Hoffman
ATTN: Donald H. Bryce
ATTN: Albert P. Bridges
ATTN: Frank H. Shelton
ATTN: T. Meagher
ATTN: Dr. D. C. Sachs
ATTN: J. C. Nickell
ATTN: J. Oscarson
ATTN: D. Williams
ATTN: R. McClellan
ATTN: E. Walsh
ATTN: Dr. P. Wieselmann
ATTN: Library

Litton Systems, Inc.
AMECOM Division
ATTN: Technical Library

Lockheed Missiles & Space Co. Inc.
ATTN: George F. Heath, Dept. 81-14
ATTN: Kevin McCarthy, 0-85-71
ATTN: Hans L. Schneemann, Dept. 81-61
ATTN: L-365, Dept. 81-20
ATTN: Philip J. Hart, Dept. 81-14
ATTN: Benjamin T. Kimura, Dept. 81-14
ATTN: D. M. Tellep, Dept. 81-01
ATTN: Dr. M. Miller
ATTN: A. O. Burford
ATTN: Technical Library

Lockheed Missiles & Space Company
ATTN: P. G. Underwood
ATTN: Technical Information Center, D/Coll.

LTV Aerospace Corporation
Vought Systems Division
ATTN: Technical Data Center

LTV Aerospace Corporation
Michigan Division
ATTN: James F. Sanson, B-2
ATTN: Technical Library

M.I.T. Lincoln Laboratory
ATTN: Leona Loughlin, Librarian A-082

Martin Marietta Aerospace
Orlando Division
ATTN: Mona C. Griffith, Lib., MP-30
ATTN: Jack M. Ashford, MP-537

Martin Marietta Corporation
Denver Division
ATTN: Paul G. Kase, Mail 8203
ATTN: Ben T. Graham, MS PO-454
ATTN: Jay R. McKee, Research Library 6617

Maxwell Laboratories, Inc.
ATTN: Richard A. Fitch
ATTN: Victor Fargo
ATTN: Technical Library

McDonnell Douglas Corporation
ATTN: Tom Ender
ATTN: Technical Library

DEPARTMENT OF DEFENSE CONTRACTORS (Continued)

McDonnell Douglas Corporation
ATTN: W. R. Spark, MS 13-3
ATTN: A. P. Venditt, MS 11-1
ATTN: Stanley Schneider
ATTN: Dr. R. J. Reck
ATTN: Dr. H. M. Berkowitz
ATTN: Technical Library Services

McDonnell Douglas Corporation
ATTN: Thomas J. Lundregan

Mission Research Corporation
ATTN: William C. Hart
ATTN: Conrad L. Longmire
ATTN: Daniel F. Higgins
ATTN: Technical Library

Mission Research Corporation
ATTN: David E. Merewether
ATTN: Larry D. Scott
ATTN: Technical Library

The Mitre Corporation
ATTN: Theodore Jarvis
ATTN: Louis Brickmore
ATTN: M. E. Fitzgerald
ATTN: Library

National Academy of Sciences
ATTN: R. S. Shane, Nat. Materials Advsy.

Northrop Corporation
ATTN: George H. Towner
ATTN: Vincent R. DeMartino
ATTN: John M. Reynolds
ATTN: Technical Library

Northrop Corporation
ATTN: Technical Library

Northrop Corporation
ATTN: Library
ATTN: David M. Pocock

Palisades Inst. for Research Services Inc.
ATTN: Records Supervisor

Perkin-Elmer Corporation
ATTN: Technical Library

Philco-Aeronut
ATTN: R. Lyons

Physics International Company
ATTN: Document Control for Bernard H. Bernstein
ATTN: Document Control for John H. Huntington
ATTN: Document Control for Technical Library
ATTN: Dr. J. Shea
ATTN: K. Childers

Procedyne Corporation
ATTN: Peter Horowitz
ATTN: Technical Library

Prototype Dev. Asso.
ATTN: T. McKinley

R & D Assoc.
ATTN: Dr. A. Field

DEPARTMENT OF DEFENSE CONTRACTORS (Continued)

R & D Associates
ATTN: Gerard K. Schlegel
ATTN: William R. Graham, Jr.
ATTN: William J. Karzas
ATTN: Charles Mo
ATTN Leonard Schlessinger
ATTN: S. Clay Rogers
ATTN. Robert A. Poll
ATTN: Richard R. Schaefer
ATTN: Technical Library

The Rand Corporation
ATTN: Cullen Crain
ATTN: Technical Library

Raytheon Company
ATTN: Library
ATTN: Gajanan H. Joshi, Radar Sys. Lab.

Raytheon Company
ATTN: James R. Weckback
ATTN: Technical Library

RCA Corporation
Government & Commercial Systems
ATTN: Technical Library

RCA Corporation
Government & Commercial Systems
ATTN: Andrew L. Warren
ATTN: Technical Library

RCA Corporation
Camden Complex
ATTN: E. Van Keuren, 13-5-2
ATTN: Technical Library

Rockwell International Corporation
ATTN: K. F. Hull
ATTN: Donald J. Stevens, FA-70
ATTN: James E. Bell, HA-10
ATTN: Technical Library

Rockwell International Corporation
Space Division
ATTN: TIC, D/41-092, AJ01

Rockwell International Corporation
ATTN: T. B. Yates

Sanders Associates, Inc.
ATTN: Moe L. Aitel, NCA 1-3236
ATTN: Technical Library

Science Applications, Inc.
ATTN: Frederick M. Tesche

Science Applications, Inc.
ATTN: William L. Chadsey

Science Applications, Inc.
ATTN: Lewis M. Linson
ATTN: B. H. Fishbine
ATTN: S. J. Dalich
ATTN: J. N. Wood
ATTN: R. Fisher
ATTN: Technical Library

DEPARTMENT OF DEFENSE CONTRACTORS (Continued)

Science Applications, Inc.
Huntsville Division
ATTN: Noel R. Byrn
ATTN: Technical Library

Science Applications, Inc.
ATTN: James R. Hill
ATTN: R. Parkinson
ATTN: Richard L. Knight

Simulation Physics, Inc.
ATTN: John R. Uglum

Simulation Physics, Inc.
ATTN: R. Little

The Singer Company
ATTN: Irwin Goldman, Eng. Management
ATTN: Technical Library

Singer Information Systems Network
ATTN: Technical Information Center

Southern Research Institute
ATTN: C. Pears

Sperry Microwave Electronics Division
Sperry Rand Corporation
ATTN: Technical Library

Sperry Rand Corporation
Univac Division
Defense Systems Division
ATTN: Technical Library

Sperry Rand Corporation
Sperry Division
Sperry Gyroscope Division
ATTN: Paul Marraffino
ATTN: Charles L. Craig, EV
ATTN: Technical Library

Sperry Rand Corporation
Sperry Flight Systems Division
ATTN: D. J. Keating
ATTN: Technical Library

Stanford Research Institute
ATTN: Philip J. Dolan
ATTN: William C. Taylor
ATTN: Arthur Lee Whitson
ATTN: George Carpenter
ATTN: Dr. G. Abrahamson
ATTN: SRI, Library, Rm. G-021

Stanford Research Institute
ATTN: MacPherson Morgan
ATTN: Technical Library

Sundstrand Corporation
ATTN: Curtis B. White

Systems, Science & Software
ATTN: Technical Library

Systems, Science & Software, Inc.
ATTN: Dr. G. Gurtman

DEPARTMENT OF DEFENSE CONTRACTORS (Continued)

Systems, Science & Software, Inc.
  ATTN: Andrew R. Wilson
  ATTN: Technical Library

Systron-Donner Corporation
  ATTN: Technical Library

Texas Instruments, Inc.
  ATTN: Donald J. Manus, MS 72
  ATTN: Gary F. Hanson
  ATTN: Technical Library

TRW Semiconductors
Division of TRW, Inc.
  ATTN: Technical Library

TRW Systems Group
  ATTN: William H. Robinette, Jr.
  ATTN: Fred N. Holmquist, MS R1-2028
  ATTN: Benjamin Sussholtz
  ATTN: Paul Molmud, R1-1196
  ATTN: Aaron H. Narevsky, R1-2144
  ATTN: A. M. Liebschutz, R1-1162
  ATTN: Lillian D. Singletary, R1-1070
  ATTN: Technical Information Center, S-1930
  ATTN: Robert M. Webb, MS R1-1150
  ATTN: Richard H. Kingsland, R1-2154
  ATTN: Dr. D. Jortner

TRW Systems Group
San Bernardino Operations
  ATTN: John E. Dahnke
  ATTN: H. S. Jensen

DEPARTMENT OF DEFENSE CONTRACTORS (Continued)

TRW Systems Group
8 cy ATTN: Technical Library

United Aircraft Corporation
Hamilton Standard Division
  ATTN: Technical Library

United Technologies Corporation
Norden Division
  ATTN: Technical Library

Victor A. J. Van Lint (Consultant)
  ATTN: V. A. J. Van Lint

Varian Associates
  ATTN: Howard R. Jory, A-109
  ATTN: Technical Library

Westinghouse Electric Corporation
Astronuclear Laboratory
  ATTN: Technical Library

Westinghouse Electric Corporation
Defense & Electronic Systems Center
  ATTN: Henry P. Kalapaca, MS 3525
  ATTN: Technical Library

Westinghouse Electric Corporation
Research & Development Center
  ATTN: Technical Library

Official Record Copy/ Lt Mac Farlane, AFWL/DYV